

JAN 11 1952

REFERENCE
FILED

(38d)

RM E51110

RM E 51 I 10

NACA RM E51110

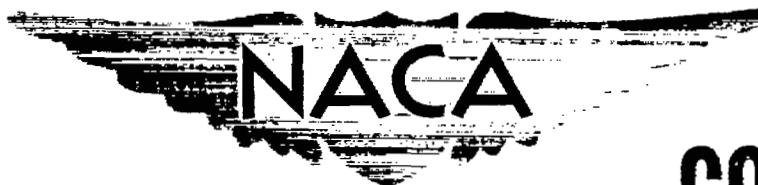
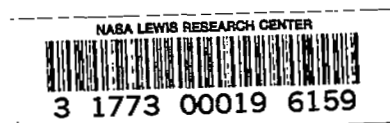


Fig. 35

COPY 1

RESEARCH MEMORANDUM



ARE F (26)

ELEVATED TEMPERATURE PROPERTIES OF TITANIUM CARBIDE

BASE CERAMALS CONTAINING NICKEL OR IRON

By A. L. Cooper and L. E. Colteryahn

Lewis Flight Propulsion Laboratory
Cleveland, Ohio

LIBRARY COPY
RETURN TO
LEWIS LIBRARY, NACA
CLEVELAND, OHIO

NATIONAL ADVISORY COMMITTEE
FOR AERONAUTICS

WASHINGTON

December 3, 1951

NATIONAL ADVISORY COMMITTEE FOR AERONAUTICS

RESEARCH MEMORANDUM

ELEVATED TEMPERATURE PROPERTIES OF TITANIUM CARBIDE

BASE CERAMALS CONTAINING NICKEL OR IRON

By A. L. Cooper and L. E. Colteryahn

SUMMARY

Titanium carbide base ceramals containing nickel or iron were investigated for elevated-temperature properties. The properties studied were oxidation, modulus of rupture, tensile strength, and thermal-shock resistance. In addition to the elevated temperature properties the metallographic structure was studied.

In oxidation, unalloyed titanium carbide and the nickel and iron ceramals were found to follow general oxide growth laws. These materials exhibited two stages of oxidation, the second approximating the parabolic growth law. Although nickel ceramals exhibited better oxidation properties than the iron ceramals, the addition of either metal to titanium carbide in general decreased the oxidation resistance; however, the oxide adherence and crack resistance of both ceramals at 1800° F and of nickel ceramals at 2000° F were greater.

Tensile tests conducted at 2000° F showed the following strengths in pounds per square inch: 13.3-weight-percent nickel ceramal, 16,150; 11.8-weight-percent iron ceramal, 12,500; highest value obtained for unalloyed titanium carbide, 16,450. Greater additions of either nickel or iron decreased the tensile strength.

Nickel or iron additions to titanium carbide greatly increased the thermal-shock resistance; nickel was found to be the more effective additive.

Microscopic study of ceramal tensile and thermal-shock fractures revealed that the path of fracture progresses approximately 50 percent intergranularly and 50 percent transgranularly.

INTRODUCTION

Since the advent of the aviation gas-turbine engine, the superalloys have been utilized in engine components subjected to the hot combustion gases. The desire to raise the operating temperature of the engine beyond

those attainable with the superalloys has created new material problems. These problems are at present being attacked by various widely different approaches. One approach is to cool the superalloys in such a manner that they may be exposed to the higher temperatures (reference 1); another is to search for a more refractory material to replace the superalloys.

Ceramic and ceramal (ceramic plus metal) materials have been investigated because of their refractory nature and because they are less strategic than superalloys. Studies of the use of cobalt, tungsten, and molybdenum as addition metals in titanium carbide base ceramals have shown promising properties for the cobalt-bonded bodies (references 2 and 3).

An investigation has been conducted at the NACA Lewis laboratory to determine the effect of additions of the less strategic metals, nickel or iron, on the properties of titanium carbide. The effects of the nickel and iron additions on microstructure and density, oxidation resistance, modulus of rupture, tensile strength, and thermal-shock resistance of titanium carbide were investigated. Bodies produced by the cold-press and the hot-press techniques were studied. The fracture paths through bodies tested in tension and thermal shock were studied metallographically in an effort to determine whether the carbide or the metal phase was controlling properties.

MATERIAL AND SPECIMEN HISTORY

The specimens evaluated in this investigation were commercially fabricated. Cold-pressed bodies were prepared with titanium carbide, containing 19.90 weight percent combined carbon, and hydrogen-reduced nickel or iron. Hot-pressed bodies were prepared with titanium carbide, containing 19.2 to 20 weight percent combined carbon, 0.25 to 0.65 free carbon, 0.05 silicon, and 0.04 iron, and with carbonyl-process nickel or iron. Proportionate amounts of these -325 mesh powders were milled together to yield specimens of the following nominal weight-percent compositions: 15, 20, 25, and 30 nickel; 10, 20, and 30 iron. The cold pressed bodies were compacted at 50,000 to 60,000 pounds per square inch at room temperature and vacuum-sintered at 2700° to 2800° F; the hot-pressed bodies were compacted at 2000 pounds per square inch at 2900° to 2970° F in graphite molds.

Chemical analyses of representative samples of the bodies are shown in table I. Because of the discrepancy between the nominal and the actual metal analyses, the average metal content based on the chemical analyses will be used throughout the text. The iron and tungsten contamination in the bodies probably occurred during the milling.

After the specimens were received from the fabricators, they were inspected for surface and internal flaws by fluorescent oil and radiographic methods, respectively. The inspection results showed all bodies to be sufficiently sound to warrant evaluation.

APPARATUS AND PROCEDURE

Metallographic Examination

Metallographic specimens were obtained by cutting a small sample from the test specimen. In order to minimize fragmentation of the tensile fracture plane by the diamond abrasive cut-off disc, nickel was plated onto the fractured surfaces prior to cutting the specimens axially. All specimens were then prepared by the usual metallographic polishing procedures for hard materials and examined at various magnifications. Murakami's reagent for the etching of carbides was used to reveal the microstructure.

Density Evaluation

The densities of samples taken from the ends of both tensile and modulus-of-rupture specimens prior to testing were determined by the method of differential weighing in air and in water. The error in these determinations was estimated to be less than ± 0.01 gram per milliliter.

Oxidation Evaluation

Oxidation specimens were prepared by sectioning rectangular prisms approximately 5/16 by 5/16 by 1/2 inch from the ends of the cold-pressed tensile specimens.

A specimen was weighed, placed upon a fire-clay brick, and heated in a conventional-type Globar muffle furnace at 1800°, 2000°, or 2200° F in a stagnant air atmosphere for times up to 150 hours. At definite intervals, the specimen was removed from the furnace, air-cooled, reweighed, and returned to the furnace for further oxidation. All handling operations were performed very carefully both to preserve the oxide as a continuous coating, if possible, and to conserve the oxide flakes if the coating spalled during cooling. The oxidation data were then calculated in terms of weight change per unit area (mgs/sq cm).

Modulus-of-Rupture Evaluation

Rectangular modulus-of-rupture specimens approximately 1/4 by 1/2 by 4 inches were prepared by finish-grinding rough bars fabricated by both the cold-press and hot-press techniques.

Evaluations were conducted at 1800°, 2000°, 2200°, and 2400° F $\pm 10^\circ$ F with the general apparatus and procedure of reference 2. The test consisted of supporting the specimen upon two silicon carbide knife edges spaced 3.5 inches apart and loading at the center through a third opposing knife edge. Oxidation of the specimens during test was minimized by placing the specimen and knife edges in a closed protective atmosphere chamber mounted within the furnace. An argon flow of 40 cubic feet per hour was used during the tests. After the specimen was placed in the atmosphere chamber, 10 minutes was allowed for the specimen to heat to the evaluation temperature prior to loading. A nominal loading rate of 2000 pounds per square inch per minute in the extreme outer fiber at the specimen midpoint was used. The specimen temperature was measured by the use of a platinum - platinum - 13-percent-rhodium thermocouple. The rupture-strength calculations were based on the original dimensions, because oxidation did not appreciably affect the dimensions.

Tensile Evaluation

Elevated-temperature tensile-strength evaluations were conducted using a conical-end specimen and the general procedure of reference 4.

The specimens were prepared by the cold-press technique and were finish-ground to a 0.5-inch diameter with a 1.25-inch gage length. The apparatus consisted of a universal hydraulic tensile machine (0.50 percent maximum machine error) fitted with an automatic-temperature-controlled commercial Globar tube furnace. The furnace was modified in order to maintain a helium atmosphere at a slight positive pressure within the furnace tube. Specimen temperature was measured with a platinum - platinum - 13-percent-rhodium thermocouple located at the center of the gage length.

Bending stresses in the specimen were minimized by room-temperature alinement of the specimen and the linkage. Measurements of misalignment were made with wire strain gages mounted on the specimen at 90° radial positions at the center of the gage length and at nominal loads of 500 and 3000 pounds per square inch. Specimen alinement was considered satisfactory when the bending stresses were less than 20 percent of the average tensile stress.

After alinement, the specimens were raised to the test temperature and soaked for 1/2 hour at a nominal load of 500 pounds per square inch. All were evaluated at 2000° $\pm 12^\circ$ F and at a nominal loading rate of 2000 pounds per square inch per minute. Since oxidation was not appreciable, the strengths were computed with the original areas.

Thermal-Shock Evaluation

$$\frac{17-2}{2} = 8$$

Thermal-shock tests were made with the apparatus and procedure of reference 4. The quenching chamber was modified to provide increased air velocity over the specimen by decreasing the inside diameter from 6 to 3 inches through a suitably designed venturi section.

Thermal-shock specimens, 2-inch diameter disks 1/4 inch thick, were prepared by the cold-press technique. The test consisted of placing the specimen in a furnace at evaluation temperature for 10 minutes, then quenching in an air stream to 70° to 80° F. The specimen was transferred from the furnace to the quenching chamber by the use of a spring-loaded holder (fig. 1). Progressive testing was carried out at 1800°, 2000°, 2200°, and 2400° ± 20° F; at each temperature the specimen was quenched 25 times for a cumulative total of 100 cycles or to failure, whichever occurred first. Quenching air was supplied to the specimen at a velocity of approximately 265 feet per second and a flow of 50 ± 2 pounds per minute at 70° to 80° F. One specimen of each composition that survived these conditions was quenched an additional 25 cycles from 2400° F in 160 ± 3 pounds of air per minute at an approximate velocity of 495 feet per second. Upon satisfactory completion of the progressive thermal-shock tests at 50 pounds per minute, and also at 160 pounds of air per minute, the specimens were inspected radiographically to determine whether internal failure had occurred.

RESULTS AND DISCUSSION

Materials Structure

The microstructures of titanium carbide base ceramals containing nickel and iron additions in the as-received condition are shown in figures 2 to 5. In all the cold-pressed and hot-pressed nickel and iron bodies it appears that some bonds exist between the carbide grains; however, the area of the bond and the number of bonds decrease as the metal content increases.

A comparison of figure 2 with 3 and figure 4 with 5 shows that the carbide grain size after sintering was much larger in the bodies prepared by the hot-press method than in the bodies prepared by the cold-press method. (This difference could reasonably be expected since the sintering temperature was higher in the hot-press method, even though the time at temperature was much shorter.)

$$\frac{36}{2} = 18$$

The degree of porosity (fig. 2 to 5) in the nickel bodies was observed to be approximately the same for the cold-pressed and hot-pressed bodies; however, in the iron bodies the hot-pressed compositions exhibited the greatest porosity. A comparison of the measured densities in table II with the calculated densities confirms this observation.

In figures 2 to 5 the carbide grains in both the nickel and iron bonded bodies show what appears to be a "cored" structure within the grain as evidenced by the differential etching characteristics across the grain. Since the cold-pressed and hot-pressed nickel bodies and the hot-pressed iron bodies were sintered at temperatures above the melting point of the respective metals (melting point of nickel 2651° F, iron 2802° F) and the cold-pressed iron bodies were sintered within 100° F of the melting point of pure iron, the sintering undoubtedly occurred in the presence of a liquid phase.

Wyman and Kelley (reference 5) and Meerson (reference 6) have established that tungsten carbide grain growth occurs in tungsten carbide - cobalt bodies when sintered in the presence of a liquid phase. These investigators found that a portion of the tungsten carbide was dissolved by the cobalt and subsequently deposited on the remaining undissolved tungsten carbide during cooling.

The "core," which is of irregular shape and not in conformance with the final grain outline, may have been undissolved titanium carbide upon which precipitation of titanium carbide from the liquid phase may have occurred. Further agreement that these "cores" may be undissolved carbide particles was found in the measurement of the size of the core. In the cold-pressed and hot-pressed bodies these measurements show the core to be of a size comparable to the larger carbide powder particle sizes that were reported to have been used by the fabricators. This coring phenomenon is much more apparent in the visual microexamination than in the photomicrographs and is also more apparent in the hot-pressed bodies.

Oxidation

The oxidation of titanium carbide and titanium carbide base ceramics containing nickel and iron was observed to follow the general growth law $w^n = kt$, proposed by Lustman and Mehl (references 7 and 8), where

- w weight gain, mg/cm²
- n reaction index
- k reaction constant
- t time in hours

By plotting weight gain as a function of time on a log-log scale (figs. 6 to 8), straight lines were obtained for the oxidation time periods investigated. The best lines were determined by application of the method of least squares for curve fitting to the experimental data

2299
(reference 9), and the reaction index n and the reaction constant k were calculated. These values for n and k are presented in table III. Changes in the reaction index n are indicative of changes in the mechanism of oxidation. For a particular material and temperature, a change to a greater value of n (n approaching the parabolic value of 2) would be beneficial to the oxidation resistance of the material because it indicates that diffusion across a barrier film is becoming the controlling mechanism, as compared to the linear growth mechanism ($n = 1$) where the interface reaction is the controlling factor, that is, where oxide growth is independent of the thickness of the reaction product. For convenience in the comparison with parabolic growth, dashed lines of slope $1/2$ ($n = 2$) representing the parabolic growth rate have been included in the figures.

Unalloyed titanium carbide (fig. 6) showed single reaction indices at both 1800° and at 2000° F, although the actual indices differed. The reaction index value n at 1800° F was 1.70 for times up to 50 hours; an increase in temperature to 2000° F caused the oxidation to become more nearly linear with a reaction index value n of 1.32 for times up to 75 hours. At these times testing was discontinued because of cracking of the oxide coating. At 2200° F, however, the oxidation was found to be a two-stage process wherein oxidation proceeded with a reaction index value n of 1.46 for the first 25 hours and then began to follow approximately the parabolic growth law for times up to 100 hours. During this second stage of oxidation, the reaction index was 2.13. The factors causing the change in the oxidation mechanism are unknown at this time.

The oxidation of unalloyed titanium carbide has been previously investigated at temperatures of 800° , 900° , and 1000° C (1472° , 1652° , and 1832° F) by Cockett and Watt (reference 10). Their data do not agree with the data of this investigation. The discrepancy probably is due to the differences in the methods used.

Nickel additions to titanium carbide (fig. 7) produced two stages of oxidation at each of the three temperatures, 1800° , 2000° , and 2200° F. The effect of nickel additions on the reaction index of titanium carbide during the first stage of oxidation at 1800° and 2000° F was to decrease the index and thereby to cause the growth rate to become more nearly linear, whereas at 2200° F the reaction index was increased and thus caused the growth rate to more nearly approach parabolic. The growth rate for the second stage of oxidation at these three temperatures was found to be approximately parabolic. A comparison of the time required to initiate the second stage of oxidation cannot be made at 1800° and 2000° F for the nickel ceramals and unalloyed titanium carbide; at 2200° F the nickel additions did not appear to have any effect, as the time was about the same as for unalloyed titanium carbide, approximately 25 hours.

The addition of nickel to titanium carbide improved the characteristics of the oxide film at 1800° and 2000° F by preventing the cracking which was noted for unalloyed titanium carbide and by increasing the adherence of the oxide coating.

The effect of iron additions on the oxidation of titanium carbide at 1800° F was to decrease the reaction index (table III and fig. 8). The iron ceramals at 1800° F did not exhibit a second stage of oxidation for the lengths of time investigated (150 hours). The addition of iron increased the oxide adherence and prevented cracking of the scale at 1800° F.

At 2000° and 2200° F the iron ceramals exhibited two stages of oxidation (fig. 8). In the first stage of oxidation the 11.8 weight percent at 2000° F and all compositions at 2200° F oxidized essentially linearly with n values ranging from 0.90 to 1.04, suggesting that the mechanism was controlled by essentially an interface reaction process. A slight increase in the reaction index (n) occurred at the second stage of oxidation at 2000° F; however, the oxide film began to crack at the long exposure times and a deviation toward more rapid oxidation could be expected (fig. 9). In the second stage of oxidation at 2200° F all of the iron compositions followed approximately the parabolic growth rate, but at 50 hours the oxide films had cracked so badly that further testing was discontinued.

The oxidation properties of a 20-weight-percent cobalt ceramal have been investigated at 1800° F by Redmond and Smith (reference 11). Their data cannot be directly compared with the nickel and iron ceramals of this investigation as they measured the increase in thickness per face; therefore, the 20-weight-percent cobalt ceramal was included in the present study to provide a basis of comparison to determine if nickel or iron could be substituted for the more strategic cobalt.

The 20-weight-percent cobalt ceramal behaved, in general, in the same manner as the nickel ceramals (fig. 10). Two stages of oxidation occurred at all temperatures for time periods to 150 hours.

The effect of iron, nickel, and cobalt on the oxidation resistance of titanium carbide is shown in figure 11 where the 50-hour weight gain is plotted against the metal content. At 1800° and 2000° F the metal additions did not improve the oxidation resistance of titanium carbide. At 2200° F the bodies with nickel additions of 13.3 and 18.2 weight percent showed less weight gain than pure titanium carbide, and higher metal additions were about equivalent. In general metal additions to titanium carbide showed a tendency to produce oxidation products that were more tightly adhering and more crack-free (fig. 9).

It would appear that in future investigations, when the effect of a metal addition to the pure carbide is considered, more accurate

comparisons might be made on the basis of measurement of depth of oxide penetration rather than weight gain to eliminate the effect of relative weights of oxidation products.

A comparison of the substitution of nickel and iron for cobalt on the basis of the 50-hour weight gain indicates that at 1800° F nickel and iron are about equivalent to cobalt. At 2000° and 2200° F the nickel is equivalent to the cobalt and both are better than iron.

A comparison of these ceramal materials with other more common heat-resisting materials is interesting. Figure 12 is a bar graph of the 50-hour weight gain for five steels tested at 2010° F (reference 12), titanium carbide, and the best ceramal compositions tested at 2000° F in this study. Although the titanium carbide and the ceramals have better oxidation resistance than a 12-chrome steel, they have poorer resistance than the other steels. Redmond and Smith (reference 11), found that addition of a tantalum-columbium-titanium carbide solid solution to titanium carbide base ceramals increased the oxidation resistance tenfold. Based on this tenfold reduction, the solid portion of the bar for the cobalt body indicates the expected weight gain for this ceramal if it contained the columbium-tantalum-titanium carbide solid solution discussed in reference 11. If the oxidation resistance of the other ceramals could be equally improved by such an addition, their new oxidation resistance would be somewhat greater than that of 17-chrome and 25-12 steels, but would still be lower than that of a 27-chrome steel.

Modulus of Rupture

The trend of the ceramals strength-temperature relation is shown by the results of testing one specimen of each composition at each temperature (fig. 13). Both nickel and iron ceramals exhibited a rapid decrease in strength with increasing temperature. (The low strengths observed at 2200° and 2400° F are of doubtful accuracy.) The general trend for nickel and iron ceramals was that of decreasing strength with increasing metal content. Anomalies exist for the hot-pressed nickel bodies tested at 1800° F and the hot-pressed iron bodies tested at 2000° F. It is believed that these values are not representative since they do not follow the established trends.

A comparison of the bodies produced by the two fabrication methods employed indicated that the conditions used in the cold-press method for nickel additions produced the better ceramals for use at 1800° to 2200° F; however, at 2400° F the strengths of the bodies are too low to permit a comparison. It is probable that further development of the fabrication techniques will result in improved body strengths.

$$\frac{15-2}{2} = 6$$

In order to determine the practicability of substituting the less strategic metals, nickel or iron, for cobalt in titanium carbide base ceramals, their elevated-temperature strengths must be compared. In figure 14, the observed strengths of the best nickel and iron bodies have been plotted against the best values reported by reference 2 for the 20-weight-percent cobalt body. If the single test values for the nickel and iron bodies can be considered as representative values, nickel and iron cannot be considered as a replacement for cobalt.

Tensile Strength

Ultimate-tensile-strength values at test temperature of 2000° F for hot-pressed titanium carbide and for cold-pressed titanium carbide base ceramals containing nickel and iron additions are presented in table IV. The values obtained for hot-pressed unalloyed titanium carbide are believed to be low since a flaw was observed in the fracture surface of each of the bodies tested. These internal flaws were not observed in the radiographic inspection.

The data in table IV are plotted in figure 15. An addition of approximately 13.3 weight percent nickel (7.9 volume percent), which was the minimum nickel content investigated, yielded the highest strength of all composition studied, but increasing nickel content above 13.3 weight percent decreased the strength linearly. Iron additions were found to be detrimental to the strength properties in all cases; the strength decreased with increasing metal content and was less than the strength of the nickel bodies.

A considerable difference was noted in the manner in which nickel and iron titanium carbide bodies failed during testing. All of the nickel compositions and the 11.8 weight-percent (7.8 volume percent) iron composition failed upon reaching the ultimate strength value; however, the 20.2- and 29.2-weight-percent (13.7 and 20.5 volume percent) iron compositions began to elongate when the ultimate strength was reached and broke at a lower load. This divergence from the characteristics of a brittle material was not as apparent in the 20.2-weight-percent bodies as in the 29.2-weight-percent bodies. Apparent small reductions in area, 0.4 to 0.8 percent, were noted for the 29.2-weight-percent bodies and examination of the specimens showed that many cracks had occurred in the test section prior to rupture (fig. 16). These cracks were not confined to the surface material but extended into the body. These phenomena indicate that a small amount of plasticity must have existed in some component of the 29.2-weight-percent iron bodies during the last stage of the test.

The path of fracture in unalloyed hot-pressed titanium carbide tested in tension at 2000° F was found to be both transgranular and

intergranular. Figure 17 shows an internal crack adjacent to the fracture in which the fracture path is approximately 60 percent transgranular. A certain amount of intergranular failure would be expected in this material because of the presence of graphite and voids in the grain boundaries; the graphite and voids decrease the effective stress-resisting area of the boundary.

(Examination of the path of fracture in titanium carbide ceramals containing nickel and iron showed that for all metal additions investigated the fracture path was about 50 percent transgranular and 50 percent intergranular.) Figures 18 and 19 show internal cracks adjacent to the fracture surface in 13.3- and 18.2-weight-percent nickel bodies, and in 20.2- and 29.2-weight-percent iron bodies, respectively. It can be seen that increasing metal content in the range investigated does not alter the fracture path. From this study, it appears that the following factors influence the fracture path: completeness of the carbide network; the "coring" effect in the carbides; and the number and distribution of voids and impurities. The function of the metal is not apparent but would be expected to influence intergranular failure whenever the metal phase is the weaker component in the body.

$$\frac{47}{2} \approx 24$$

Thermal Shock

The results of the thermal-shock evaluation are presented in table V and figure 20. The addition of either nickel or iron to titanium carbide improved the thermal-shock resistance. Pure titanium carbide failed at a temperature of 1800° F after a maximum of 9 quenching cycles, whereas the bodies containing metal did not fail until 2400° F was reached and a minimum of $85\frac{1}{2}$ cumulative quenching cycles had been completed. Of the two addition metals, nickel gave better shock resistance. Bodies containing from 13.3 to 22.7 weight percent of nickel (7.9 to 14.1 volume percent) did not fail under the most severe testing conditions used, whereas bodies containing iron failed at 2400° F after a cumulative total of 85 to 97 cycles when quenched with 50 pounds of air per minute. The 20.2-weight-percent (13.7 volume percent) iron bodies appeared to be slightly more resistant than the other iron compositions.

The 28.3-weight-percent (18.0 volume percent) nickel bodies were found to contain a fine network of internal cracks upon radiographic inspection following completion of testing at 2400° F with a 50-pound-per-minute air quench. (Figure 21 shows the fine network of cracks in the bodies as shown radiographically.) Metallographic examination of these bodies revealed that they had been so badly shattered during the test that the fracture path could not be traced.

$$\frac{16-2}{2} = 7$$

The path of fracture after shock tests, in titanium carbide base ceramals containing iron, was found to be approximately 50 percent

transgranular and 50 percent intergranular. No significant trend with increasing metal content in the path of fracture in these bodies was noted. Similarity in the fracture paths in bodies tested in tension and in thermal shock would be expected, since Norton (reference 13) has shown that failure in disks and in spheres on sudden cooling is caused by tension.

SUMMARY OF RESULTS

The following results were obtained from a determination of the elevated-temperature properties and characteristics of titanium carbide base ceramals containing nickel or iron.

1. In oxidation tests, unalloyed titanium carbide and the nickel and iron ceramals were found to follow general oxide growth laws. These materials exhibited two stages of oxidation, the last stage approximating the parabolic growth law. In general, nickel ceramals were found to exhibit better oxidation properties than the iron ceramals and addition of either nickel or iron to titanium carbide decreased the oxidation resistance; however, both ceramals at 1800° F and nickel ceramals at 2000° F increased the oxide adherence and crack resistance.

2. At a temperature of 2000° F the 13.3-weight-percent nickel ceramal had an average tensile strength of 16,150 pounds per square inch, whereas the 11.8-weight-percent iron ceramal had an average tensile strength of 12,500 pounds per square inch. Further nickel or iron additions to titanium carbide decreased the tensile strength. The highest value obtained for unalloyed titanium carbide was 16,450 pounds per square inch.

3. Ceramals containing 13.3 to 22.7 weight percent nickel survived 100 cycles of thermal-shock testing; however, the iron ceramals failed in 85 to 97 cycles. The 20.2-weight-percent iron ceramal was found to be slightly better than the other iron compositions. The addition of either metal to titanium carbide greatly increased the thermal shock resistance.

4. Microscopic study of ceramal tensile and thermal-shock fractures revealed that the path of fracture progresses approximately 50 percent intergranularly and 50 percent transgranularly.

Lewis Flight Propulsion Laboratory
National Advisory Committee for Aeronautics
Cleveland, Ohio.

REFERENCES

1. Ellerbrock, Herman H.: N.A.C.A. Investigations of Gas-Turbine-Blade Cooling. Jour. Aero. Sci., vol. 15, no. 12, Dec. 1948, pp. 721-730.
2. Deutsch, George C., Repko, Andrew J., and Lidman, William G.: Elevated-Temperature Properties of Several Titanium Carbide Base Ceramals. NACA TN 1915, 1949.
3. Whitman, M. J., and Repko, A. J.: Oxidation of Titanium Carbide Base Ceramals Containing Molybdenum, Tungsten, and Cobalt. NACA TN 1914, 1949.
4. Hoffman, Charles A., Ault, G. Mervin, and Gangler, James J.: Initial Investigation of Carbide-Type Ceramal of 80-Percent Titanium Carbide Plus 20-Percent Cobalt for Use as Gas-Turbine-Blade Material. NACA TN 1836, 1949.
5. Wyman, L. L., and Kelley, F. C.: Cemented Tungsten Carbide; a Study of the Action of the Cementing Material. Trans. A.I.M.E., Inst. Metals Div., 1931, pp. 208-226.
6. Meerson, G. A., Zverev, G. L., and Osinovskaya, B. Ye.: Investigation of Behavior of Titanium Carbide in Cemented Carbide Alloys. Trans. No. 1642, Henry Brucher Tech. Trans. Service, 1944. (Trans. from Zhurnal Prikladnoi Khimii, vol. 13, no. 1, 1940, pp. 66-75).
7. Lustman, B.: Discussion of The Transition State Theory of the Formation of Thin Oxide Films on Metals by E. A. Gulbransen. Trans. Electro-chem. Soc., vol. 83, 1943, pp. 313-315.
8. Lustman, B., and Mehl, R. F.: Rate of Growth of Intermediate Alloy Layers in Structurally Analogous Systems. Trans. A.I.M.E., Metals Div., vol. 147, 1942, pp. 369-395.
9. Mills, Frederick Cecil: Statistical Methods. Henry Holt and Co. (New York), 1938, p. 270.
10. Cockett, G. H., and Watt, W.: Reaction of Carbides with Gases at Elevated Temperatures. Pt. I. Behavior in Oxidizing Atmospheres. Tech. Note Met. 124, British R. A. E., April 1950.
11. Redmond, J. C., and Smith, E. N.: Cemented Titanium Carbide. Trans. A.I.M.E., Metals Div., vol. 185, 1949, pp. 987-993.
12. Heindlhofer, K., and Larsen, B. M.: Resistance to Scaling, Ch. 17-B, The Book of Stainless Steels, Ernest E. Thum, ed., Am. Soc. Metals (Cleveland), 2d ed., 1935, pp. 552-553.

13. Norton, F. H.: Refractories. McGraw-Hill Book Co., Inc., 2nd ed., p. 465.


2299

TABLE I - CHEMICAL COMPOSITION OF TITANIUM CARBIDE BASE CERAMALS

Specimen number	Metal addition				Titanium (percent)	Chemical analysis					
	Nominal (weight percent)	Calculated average				Nickel (percent)	Total carbon (percent)	Combined carbon (percent)	Iron (percent)	Tungsten (percent)	Method of fabrication
		(weight percent)	(volume percent)	Nickel and iron (volume percent)							
Nickel addition											
304 305 306	15	13.34	7.91	9.99	63.28 63.31 63.11	13.58 13.25 13.20	16.00 16.17 16.41	14.67 14.82 15.22	2.38 2.36 2.13	3.70 3.66 3.60	Cold press Do. Do.
307 309	15	13.52	8.01	9.25	65.03 65.15	13.22 13.82	15.71 15.69	13.54 13.68	1.70 2.00	None do.	Hot press Do.
3P4 3P5	20	18.18	11.06	12.91	58.19 58.19	17.71 18.68	15.03 14.08	13.97 13.02	3.06 2.30	3.98 3.64	Cold press Do.
3P7 3P10	20	18.76	11.38	12.32	61.50 62.24	18.73 18.79	14.74 15.05	13.00 13.28	1.43 1.30	None do.	Hot press Do.
3Q4 3Q6	25	22.70	14.08	15.45	56.96 56.54	22.70 22.89	13.96 14.06	13.05 13.20	1.85 2.05	2.32 2.24	Cold press Do.
3Q7 3Q10	25	20.14	12.32	13.52	59.62 61.11	20.56 19.72	14.39 14.69	12.69 12.60	2.03 1.45	None do.	Hot press Do.
3R4 3R6	30	28.29	18.04	19.27	53.50 52.43	27.57 29.01	13.93 13.67	13.06 12.76	1.52 1.90	0.75 0.68	Cold press Do.
3R7 3R9	30	25.74	16.19	17.29	55.46 56.44	25.92 25.56	13.79 13.80	11.95 11.58	1.70 1.40	None do.	Hot press Do.
Iron addition											
3S5 3S6	10	11.84	7.75	(a) (a)	64.74 64.16	(a) (a)	16.21 15.93	15.34 15.04	11.45 12.22	5.34 5.37	Cold press Do.
3S7 3S9	10	10.97	7.16	(a) (a)	68.11 69.30	(a) (a)	16.74 17.35	14.34 14.66	12.05 9.90	None do.	Hot press Do.
3T4 3T5 3T6	20	20.17	13.66	(a) (a) (a)	59.62 59.44 59.83	(a) (a) (a)	15.13 15.13 15.12	14.15 14.17 14.17	20.00 20.22 20.30	4.33 4.43 4.02	Cold press Do. Do.
3T7 3T8	20	20.15	13.84	(a) (a)	59.57 63.13	(a) (a)	14.66 14.90	13.51 13.58	21.80 18.50	None do.	Hot press Do.
3U5 3U6	30	29.18	20.51	(a) (a)	52.92 54.57	(a) (a)	13.88 13.35	12.40 11.80	30.15 28.20	2.01 3.95	Cold press Do.
3U7 3U10	30	21.74	14.81	(a) (a)	56.01 61.07	(a) (a)	14.46 14.59	12.92 12.76	23.00 20.48	None do.	Hot press Do.

^aNickel not analyzed.

TABLE II - DENSITY OF TITANIUM CARBIDE BASE CERAMALS

Specimen	Average metal addition (weight percent)	Density		Method of fabrication 
		Calculated ^a (gram/ml)	Measured (gram/ml)	
Nickel addition				
304	13.3	5.34	5.33	Cold press
305			5.33	Do.
306			5.33	Do.
3011			5.37	Do.
3013			5.37	Do.
307	13.5	5.19	5.15	Hot press
308			5.22	Do.
3P4	18.2	5.59	5.51	Cold press
3P5			5.49	Do.
3P6			5.51	Do.
3P12			5.49	Do.
3P13			5.49	Do.
3P7	18.8	5.31	5.26	Hot press
3P8			5.20	Do.
3Q4	22.7	5.62	5.59	Cold press
3Q5				Do.
3Q6				Do.
3Q7	20.1	5.35	5.42	Hot press
3Q8			5.43	Do.
3R4	28.3	5.74	5.68	Cold press
3R5				Do.
3R7	25.7	5.47	5.48	Hot press
3R8			5.54	Do.
Iron addition				
3S4	11.8	5.35	5.34	Cold press
3S5			5.33	Do.
3S6			5.34	Do.
3S12			5.33	Do.
3S14			5.32	Do.
3S7	11.0	4.99	4.66	Hot press
3S9			4.71	Do.
3T4	20.2	5.41	5.53	Cold press
3T5			5.53	Do.
3T6			5.52	Do.
3T8	20.2	5.34	4.86	Hot press
3T10			4.81	Do.
3U4	29.2	5.47	5.65	Cold press
3U5			5.62	Do.
3U6			5.71	Do.
3U13			5.84	Do.
3U14			5.91	Do.
3U7	21.7	5.43	5.04	Hot press
3U9			5.07	Do.

^a Computations based on assumption of mechanical mixture of constituents and on average chemical analysis.

TABLE III - OXIDATION VALUES FOR GENERAL EQUATION $w^n = kt$ FOR

TITANIUM CARBIDE BASE CERAMALS

[First line of entries under each metal addition is first stage of oxidation;
second line is second stage.]

Metal addition (weight percent)	Reaction index n	Reaction constant k	Reaction index n	Reaction constant k	Reaction index n	Reaction constant k	Indicated times for change in oxidation rate (hr)		
	Test temperature °F						Test temperature (°F)		
	1800		2000		2200		1800	2000	2200
Unalloyed titanium carbide									
0	1.70	3.53	1.32	3.36	1.46 2.13	27.79 574.38	None	None	25
Nickel									
13.3	1.41	2.42	1.29	5.58	1.65	45.27	75	20	22
	1.84	12.54	1.90	52.94	2.04	242.78			
18.2	1.42	3.08	1.22	5.46	1.81	95.24	75	11	25
	1.88	18.84	1.80	36.42	2.00	242.78			
22.7	1.46	3.90	1.17	4.90	1.86	168.55	50	20	21
	1.93	22.08	2.10	181.92	2.15	670.24			
28.3	1.59	5.76	1.18	4.60	1.91 ^a	214.68 ^a	50	19	25 ₀ ^b
	1.88	16.70	2.01	108.12	2.35 ^a 1.95 ^b	1882.9 ^a 252.3 ^b			
Iron									
11.8	1.20	1.12	0.97	2.55	0.94	7.64	None	12	12
			1.65	27.76	2.00	1195.3	None		
20.2	1.48	3.78	1.18	5.07	0.90	8.86	None	14	6
			1.74	37.81	1.97	824.4	None		
29.2	1.57	6.02	1.45	13.82	1.04	15.97	None	18	7
			1.75	41.72	1.99	1186.4			
Cobalt									
20	1.22	1.50	1.50	10.69	1.48	37.78	56	25	15
	1.83	13.23	1.80	39.15	2.44	2367.4			

^aValues for intersecting lines.

^bValues for straight line.

TABLE IV - TENSILE STRENGTH OF TITANIUM CARBIDE
BASE CERAMALS CONTAINING NICKEL AND IRON AT
2000° F AND LOADING RATE OF 2000 POUNDS
PER SQUARE INCH PER MINUTE

Specimen number	Average metal addition		Ultimate tensile strength (lb/sq in.) (a)	
	(Weight percent)	(Volume percent)	Observed	Average
Titanium carbide				
3A4 6	0 0	0 0	14,400 ^b 16,450 ^b	15,400
Nickel addition				
304 5 6	13.3	7.9	13,750 17,100 17,600	16,150
3P4 5 6	18.2	11.1	15,250 14,800 14,500	14,850
3Q4 5 6	22.7	14.1	19,800 ^c 13,600 12,500	13,100 ^d
3R4 5 6	28.3	18.0	11,200 10,900 12,800	11,650
Iron addition				
3S4 5 6	11.8	7.8	12,350 12,750 12,350	12,500
3T4 5 6	20.2	13.7	8,600 8,200 7,900	8,250
3U4 5 6	29.2	20.5	5,700 5,800 5,700	5,750



^aValues rounded to nearest 50 lb/sq in.

^bFlaw at break.

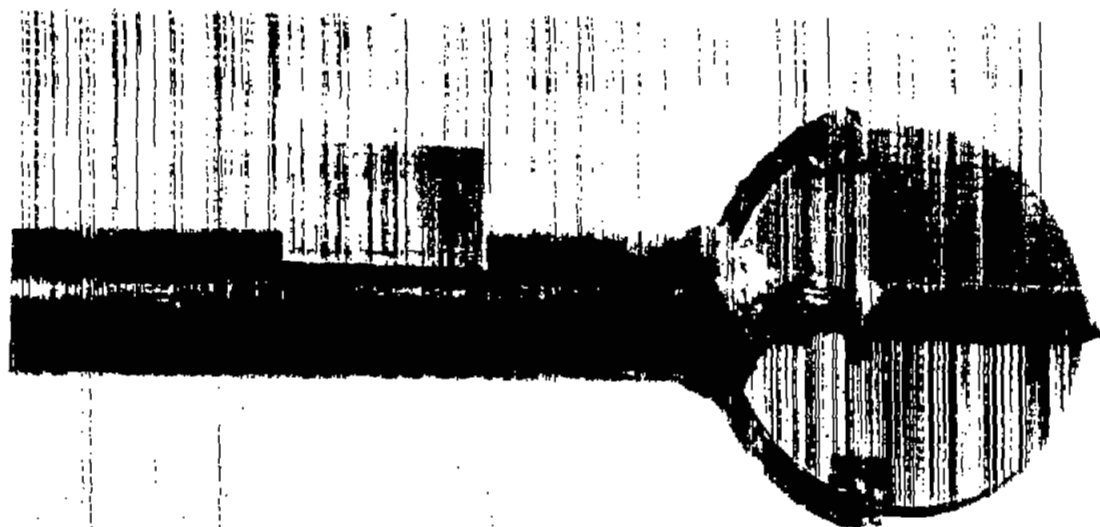
^cLoading rate, 4000 lb/sq in./min.

^dAverage of values for 3Q5 and 3Q6

TABLE V - THERMAL-SHOCK EVALUATION OF TITANIUM CARBIDE BASE
CERAMALS AND HOT-PRESSED TITANIUM CARBIDE

Specimen number	Average metal addition		Number of cycles completed					Total number of cycles	Radiographic inspection results
	Weight (percent)	Volume (percent)	50 lb air/min quenched from °F				160 lb air/min quenched from		
			1800	2000	2200	2400	2400° F		
Titanium carbide									
3A13	0	0	2					2	None
3A14			9					9	Do.
3A15			1					$\frac{1}{2}$	Do.
3A16			2					$\frac{1}{2}$	Do.
3A17			4					4	Do.
3A18			1					1	Do.
			2					2	Do.
Nickel addition									
3O2	13.3	7.9	25	25	25	25	25	125	Satisfactory
3O3								100	Do.
3P1	18.2	11.1	25	25	25	25	25	125	Satisfactory
3P2								100	Do.
3P3								100	Do.
3Q1	22.7	14.1	25	25	25	25	25	125	Satisfactory
3Q2								100	Do.
3Q3								100	Do.
3R1	28.3	18.0	25	25	25	25		100	Visible crack plus fine cracks Network of fine cracks Network of fine cracks
3R2								100	
3R3								100	
Iron addition									
3S2	11.8	7.8	25	25	25	18		93	Radial crack plus fine cracks
3S3						17		92	Radial crack plus fine crack
3T1	20.2	13.7	25	25	25	22		97	Three radial cracks
3T2						18		93	Radial crack
3T3						18			Radial crack
3U1	29.2	20.5	25	25	25	$10\frac{1}{2}$		$85\frac{1}{2}$	None
3U2						15		90	Radial crack
3U3						$17\frac{1}{2}$		$92\frac{1}{2}$	None

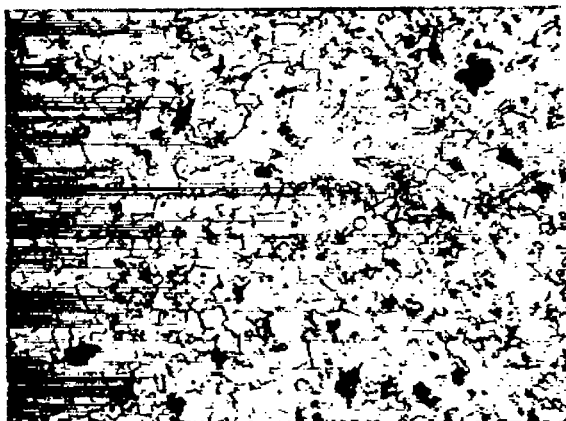




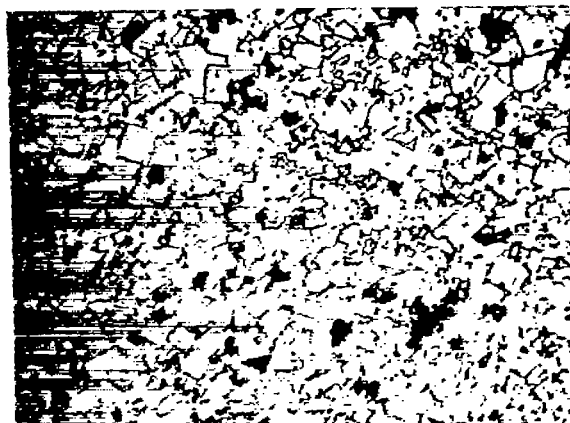
NACA
C-23687

Figure 1. - Thermal-shock-specimen holder.

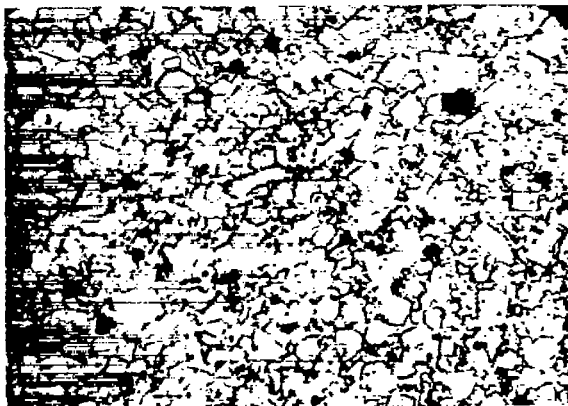
2299



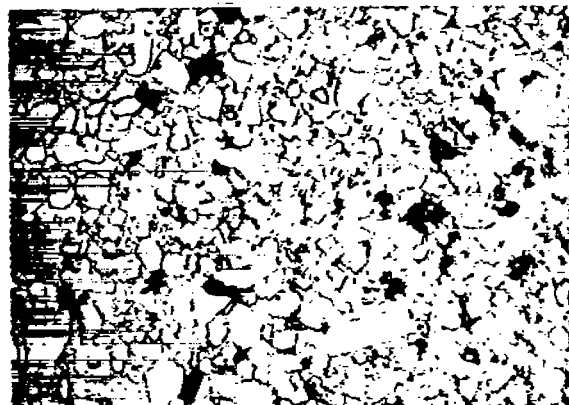
(a) 13.3 weight percent nickel (7.9 volume percent)



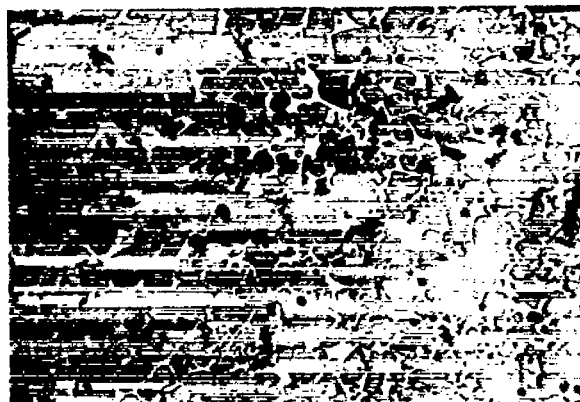
(b) 18.2 weight percent nickel (11.1 volume percent)



(c) 22.7 weight percent nickel (14.1 volume percent)



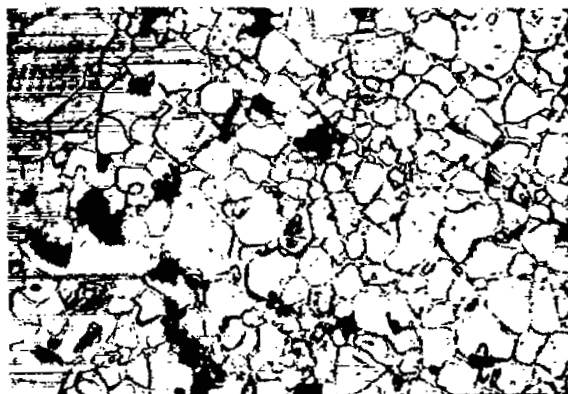
(d) 28.3 weight percent nickel (18.0 volume percent)



(e) 28.3 weight percent nickel, unetched

NACA
C-28380

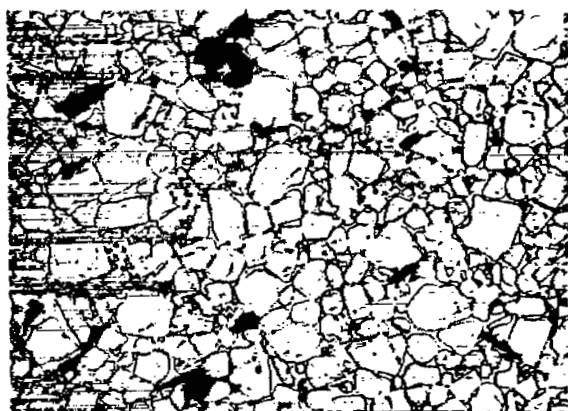
Figure 2. - Cold-pressed titanium carbide base ceramals with nickel in as-received condition. Etched with Murakami's reagent. X600.



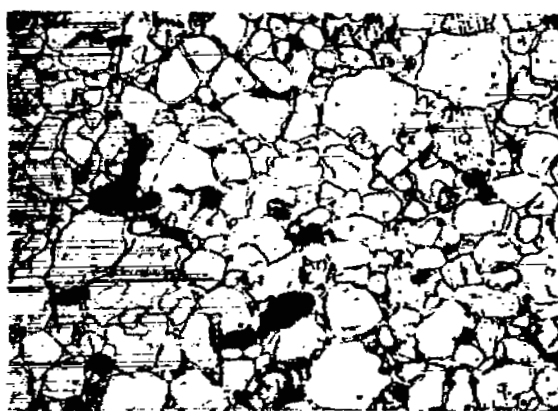
(a) 13.5 weight percent nickel (8.0 volume percent)



(b) 18.8 weight percent nickel (11.4 volume percent)



(c) 20.1 weight percent nickel (12.3 volume percent)

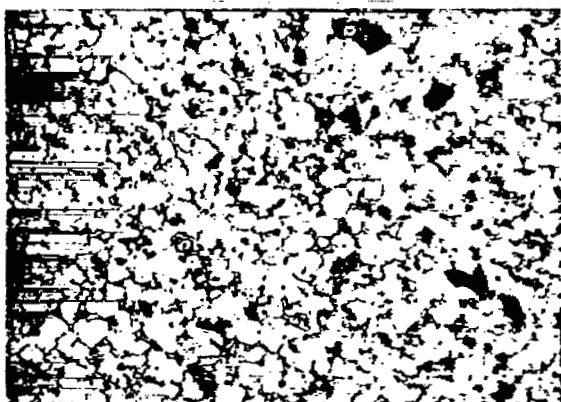


(d) 25.7 weight percent nickel (16.2 volume percent)

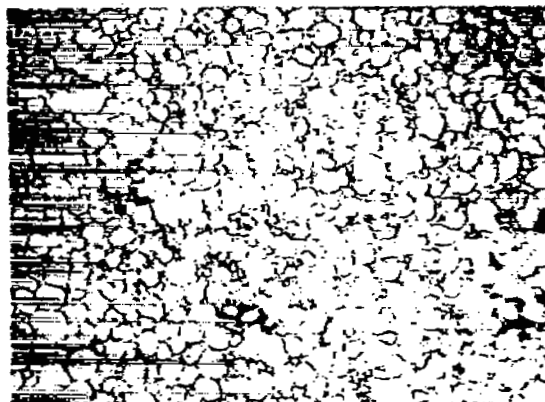
NACA
C-28381

Figure 3. - Hot-pressed titanium carbide base ceramals with nickel in as-received condition. Etched with Murakami's reagent. X600.

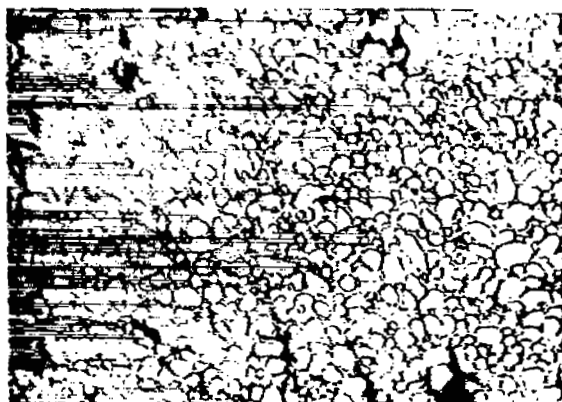
2299



(a) 11.8 weight percent iron (7.8 volume percent)



(b) 20.2 weight percent iron (13.7 volume percent)

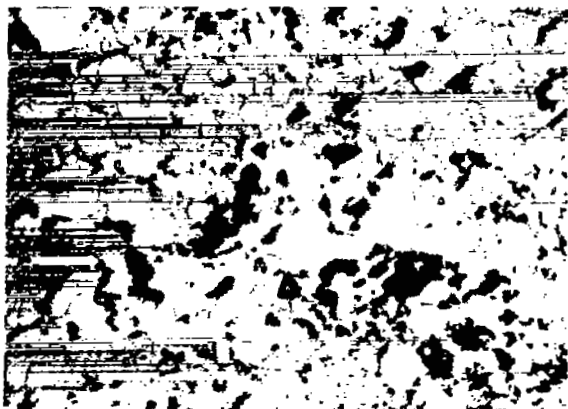


(c) 29.2 weight percent iron (20.5 volume percent)



(d) 29.2 weight percent iron, unetched

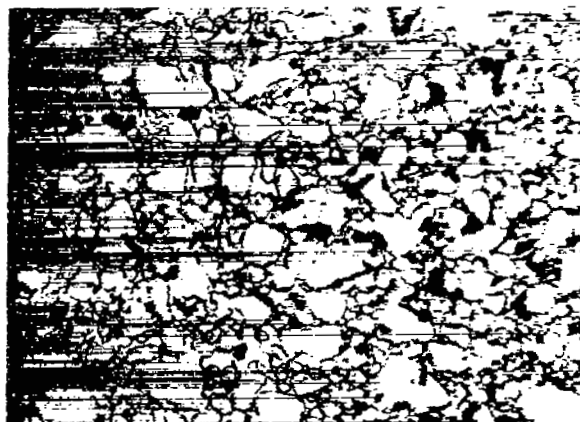
Figure 4. - Cold-pressed titanium carbide base ceramals with iron in as-received condition. Etched with Murakami's reagent. X600.



(a) 11.0 weight percent iron (7.2 volume percent)



(b) 20.2 weight percent iron (13.6 volume percent)



(c) 21.7 weight percent iron (14.8 volume percent)

NACA
C-28383

Figure 5. - Hot-pressed titanium carbide base ceramals with iron in as-received condition. Etched with Murakami's reagent. X600.

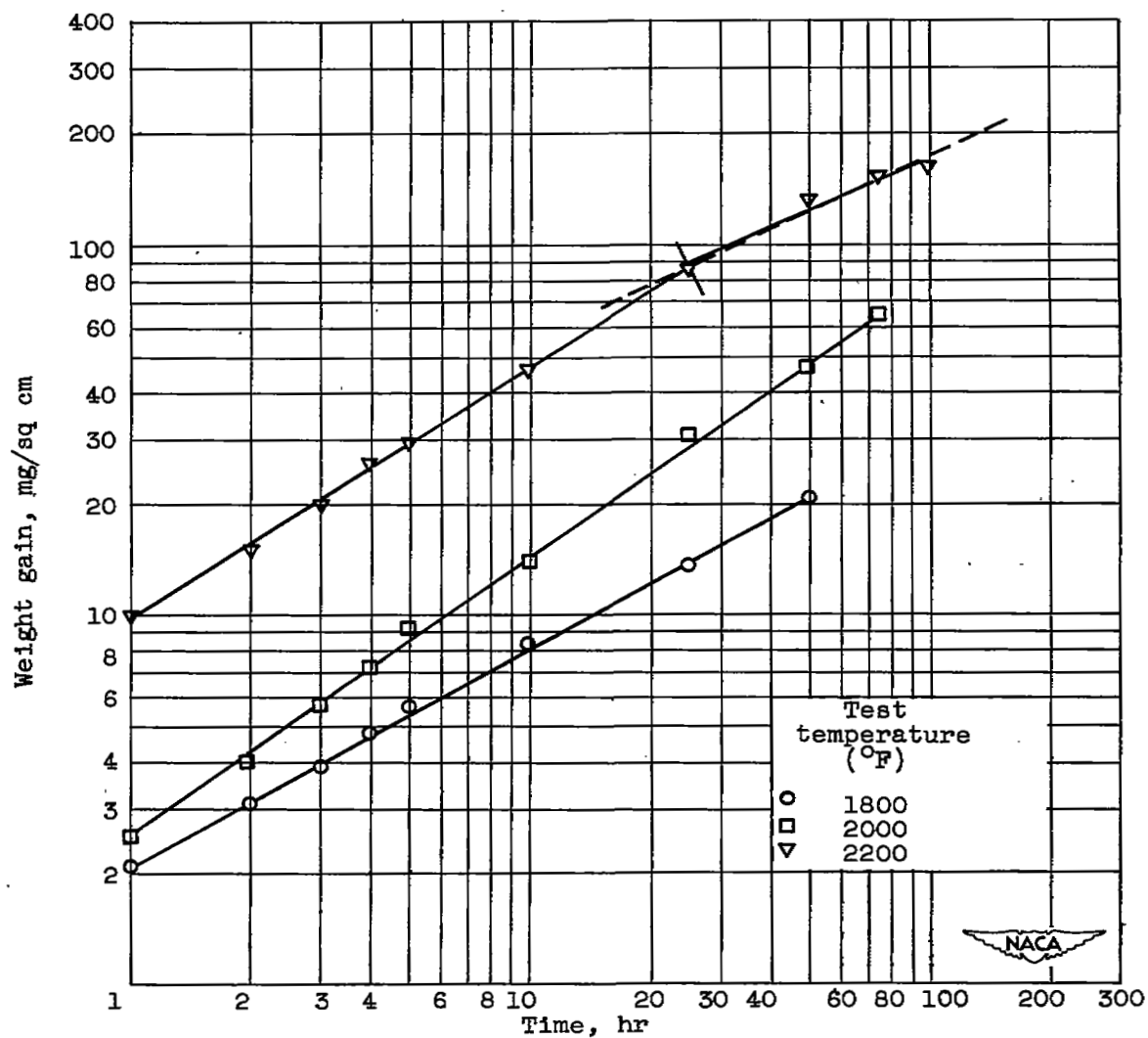
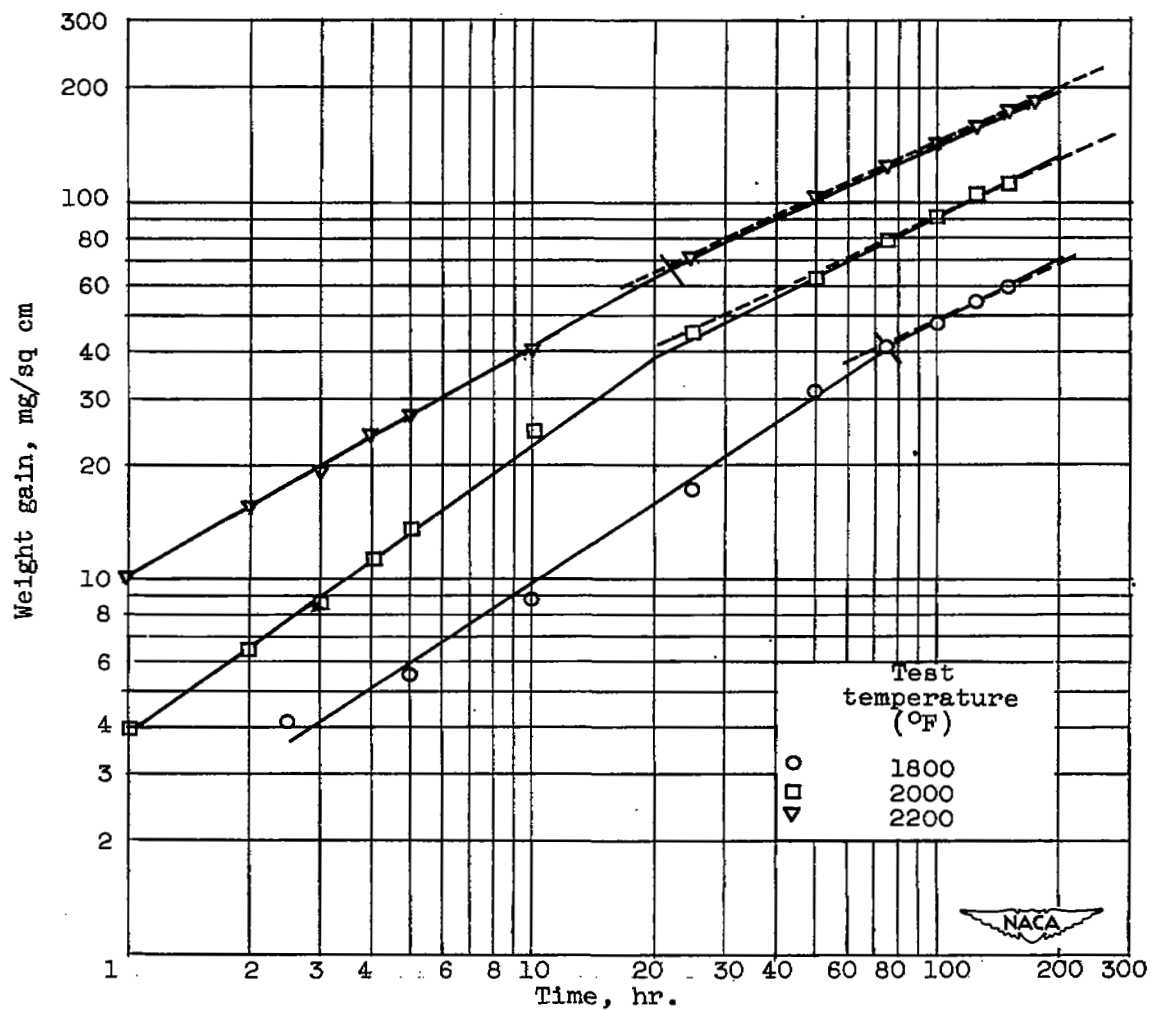
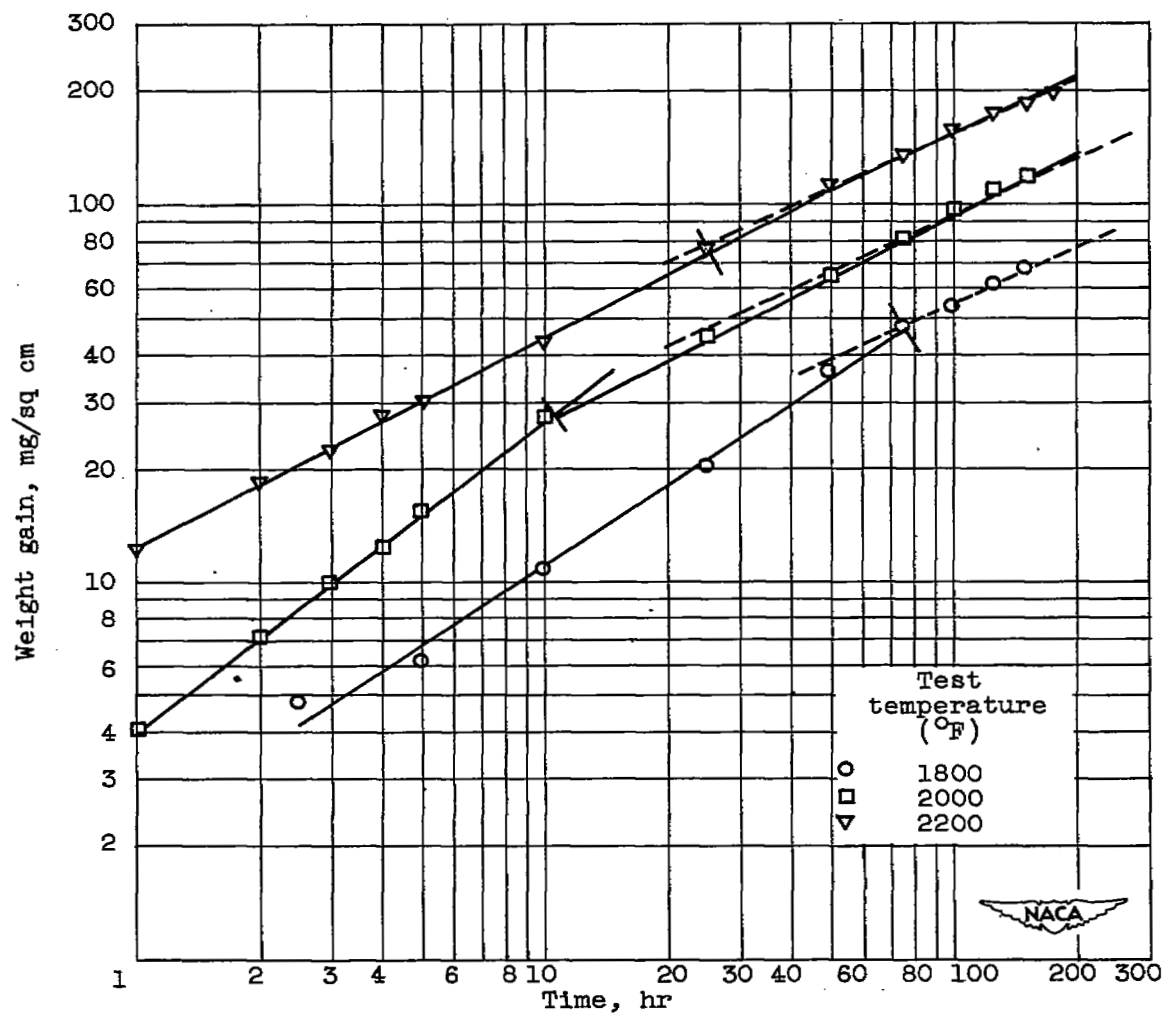


Figure 6. - Oxidation of unalloyed titanium carbide. (Dashed curve indicates parabolic growth.)



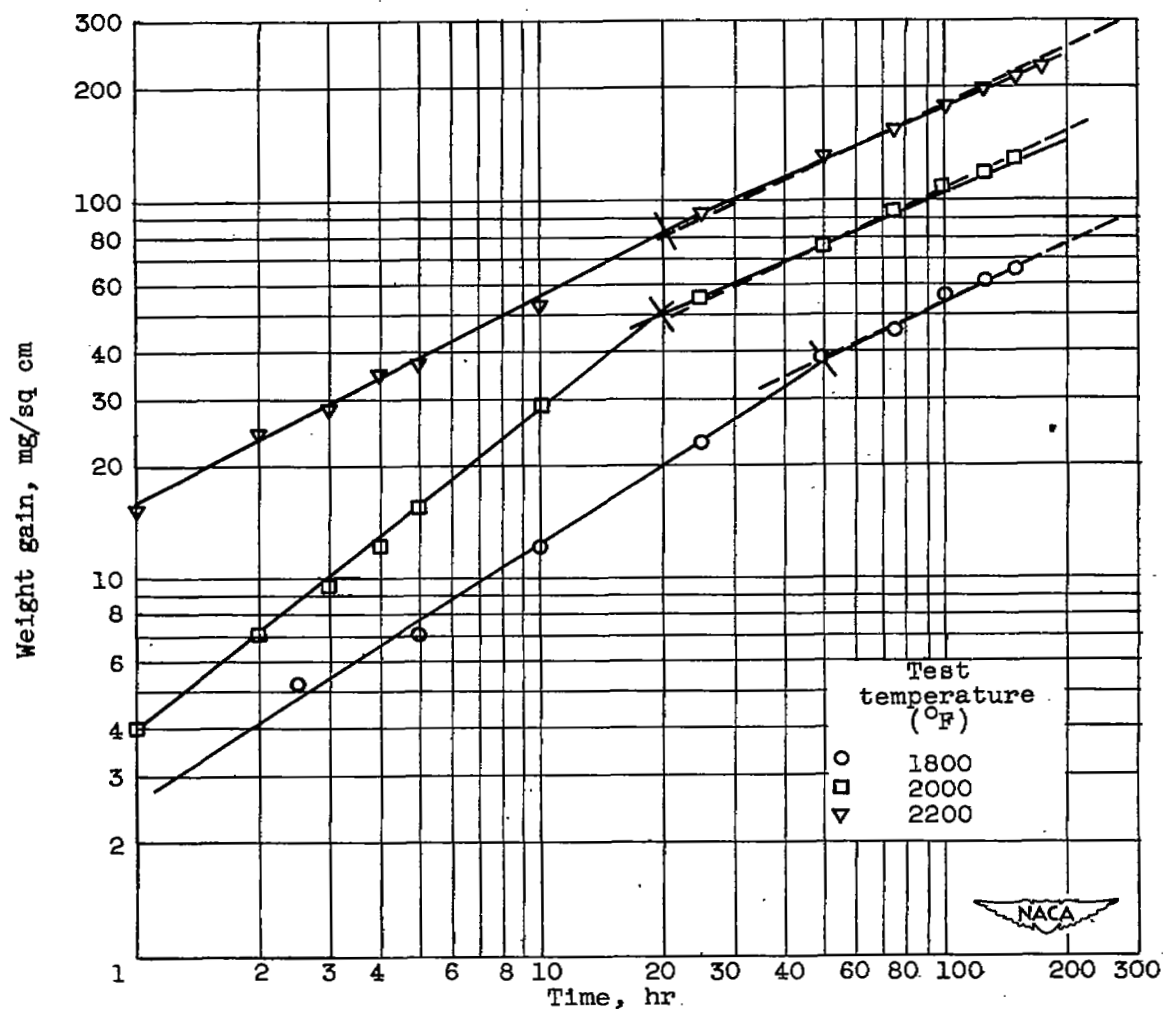
(a) 13.3 weight percent nickel.

Figure 7. - Oxidation of titanium carbide base ceramals containing nickel. (Dashed curve indicates parabolic growth.)



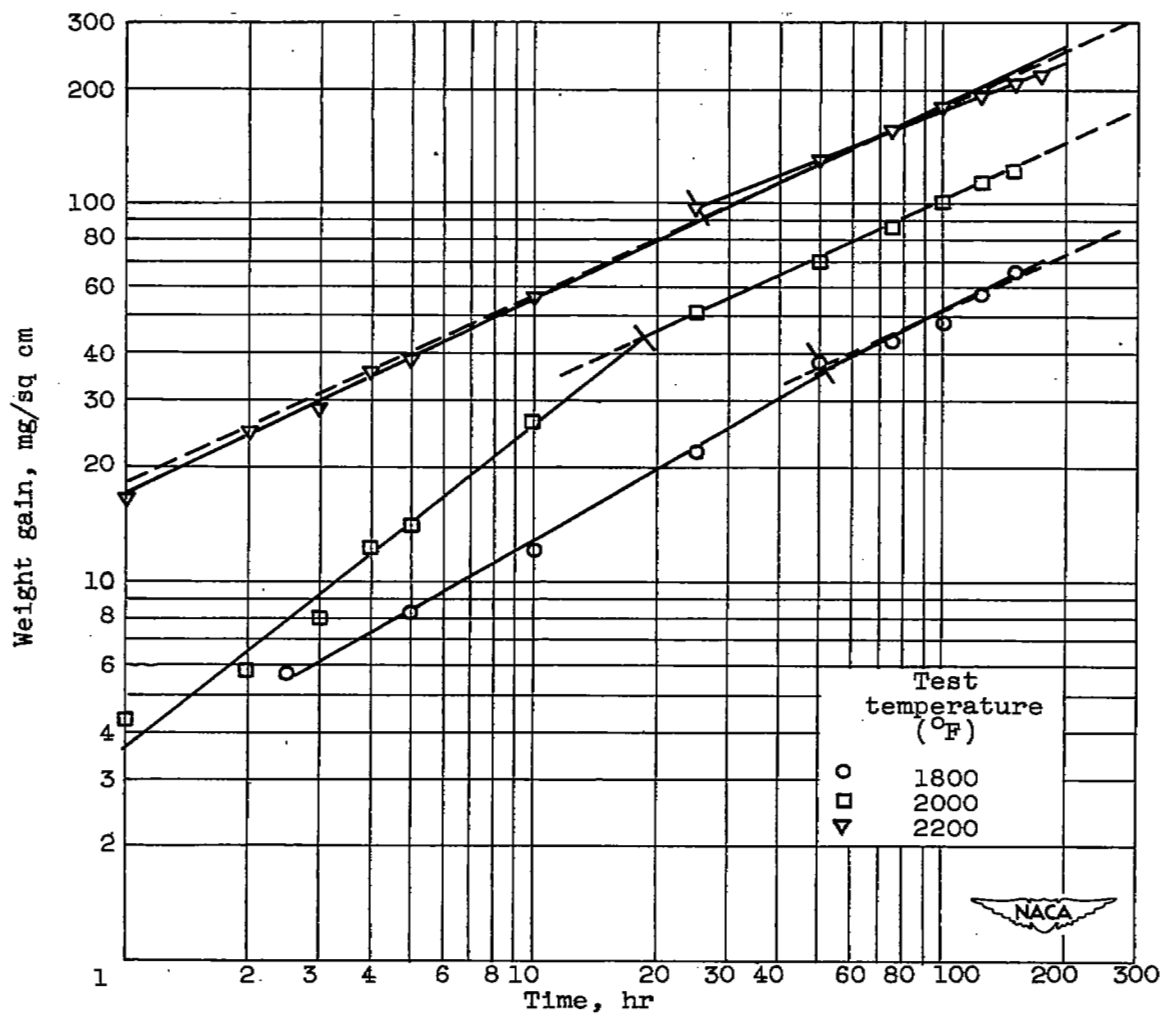
(b) 18.2 weight percent nickel.

Figure 7. - Continued. Oxidation of titanium carbide base ceramals containing nickel. (Dashed curve indicates parabolic growth.)



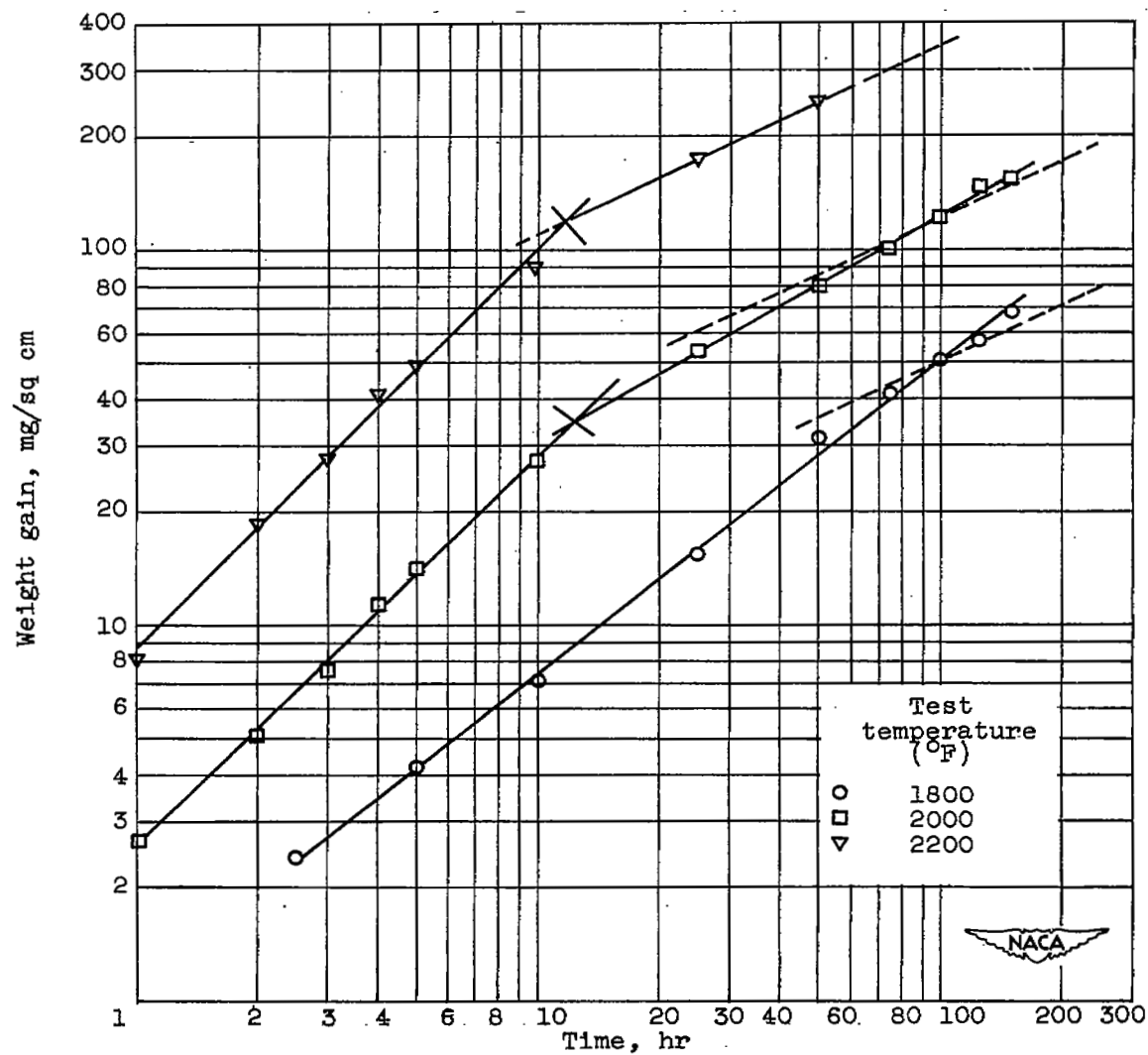
(c) 22.7 weight percent nickel.

Figure 7. - Continued. Oxidation of titanium carbide base ceramals containing nickel. (Dashed curve indicates parabolic growth.)



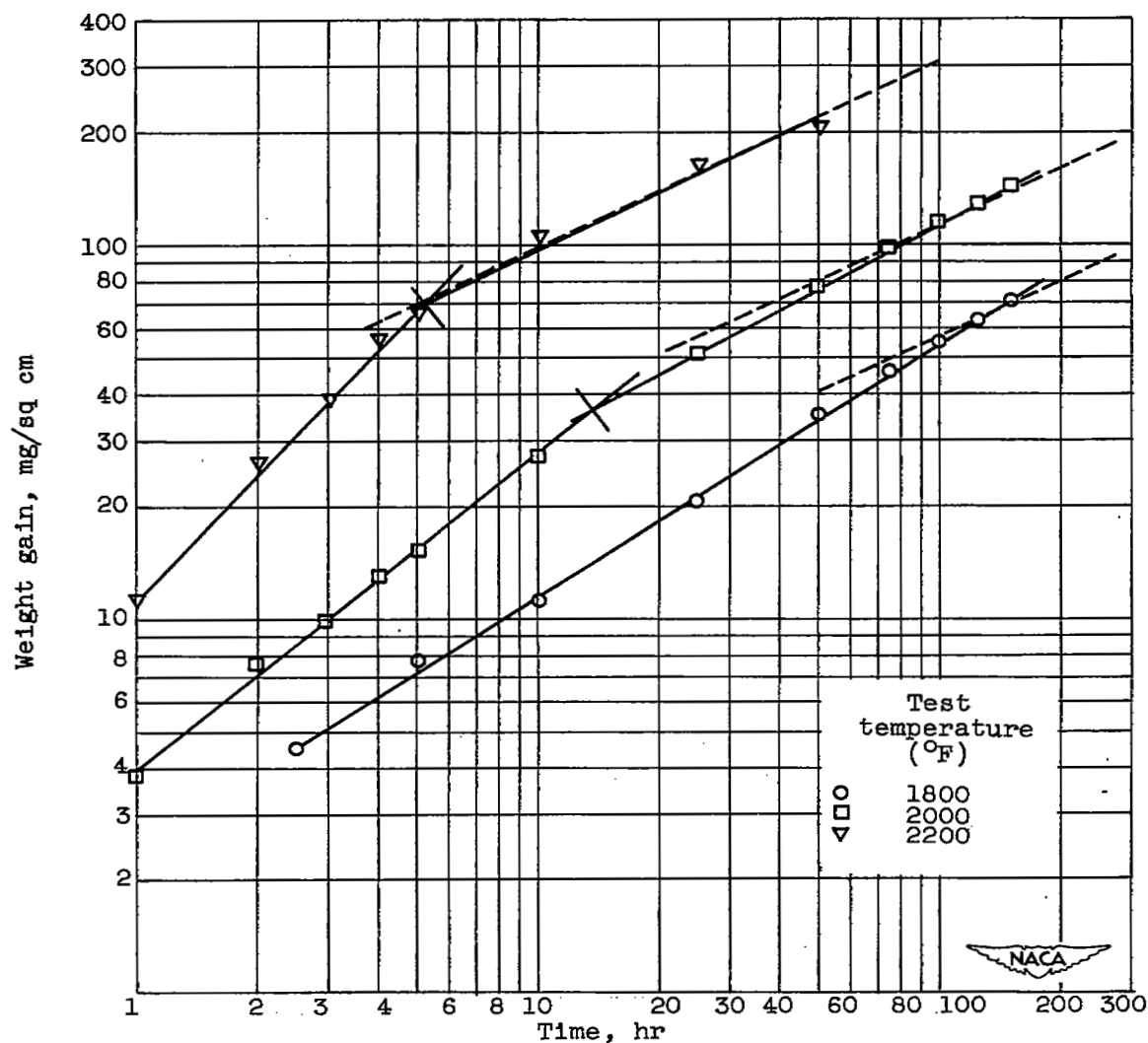
(d) 28.3 weight percent nickel.

Figure 7. - Concluded. Oxidation of titanium carbide base ceramals containing nickel. (Dashed curve indicates parabolic growth.)



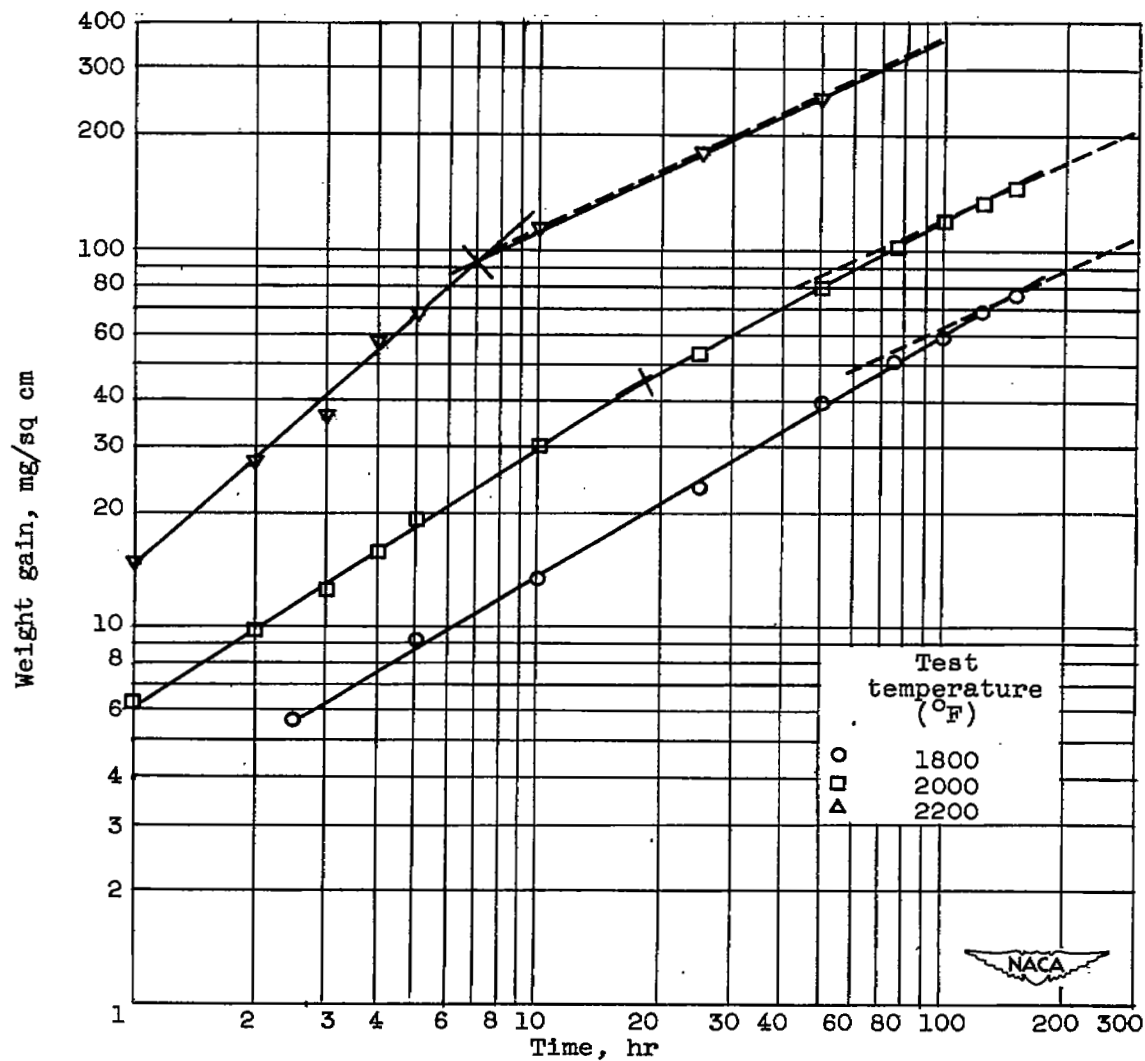
(a) 11.8 weight percent iron.

Figure 8. - Oxidation of titanium carbide base ceramals containing iron.
(Dashed curve indicates parabolic growth.)



(b) 20.2 weight percent iron.

Figure 8. - Continued. Oxidation of titanium carbide base ceramals containing iron. (Dashed curve indicates parabolic growth.)



(c) 29.2 weight percent iron.

Figure 8. - Concluded. Oxidation of titanium carbide base ceramals containing iron. (Dashed curve indicates parabolic growth.)



Surface



Transverse Section



Titanium Carbide	20	13.3	18.2	22.7	28.3	11.8	20.2	29.2 weight percent
	Cobalt	Nickel	Nickel	Nickel	Nickel	Iron	Iron	Iron

(a) Oxidation temperature, 2000° F; oxidation times: titanium carbide, 75 hours; rest of specimens, 150 hours. Outer oxide shell on titanium carbide broke away on sectioning and is not shown.

Figure 9. - Oxidation of titanium carbide base ceramics after 150 hours in still air. X2.



Surface



Transverse Section



Titanium Carbide	20 Cobalt	29.2 Iron	18.2 Nickel	22.7 Nickel	28.3 Nickel	11.8 Iron	20.2 Iron	13.3 Weight percent Nickel
------------------	-----------	-----------	-------------	-------------	-------------	-----------	-----------	----------------------------

(b) Oxidation temperature, 2200° F; oxidation times: titanium carbide 100 hours; iron, 50 hours; nickel and cobalt, 150 hours.

Figure 9. - Concluded. Oxidation of titanium carbide base ceramics after 150 hours in still air. X2.

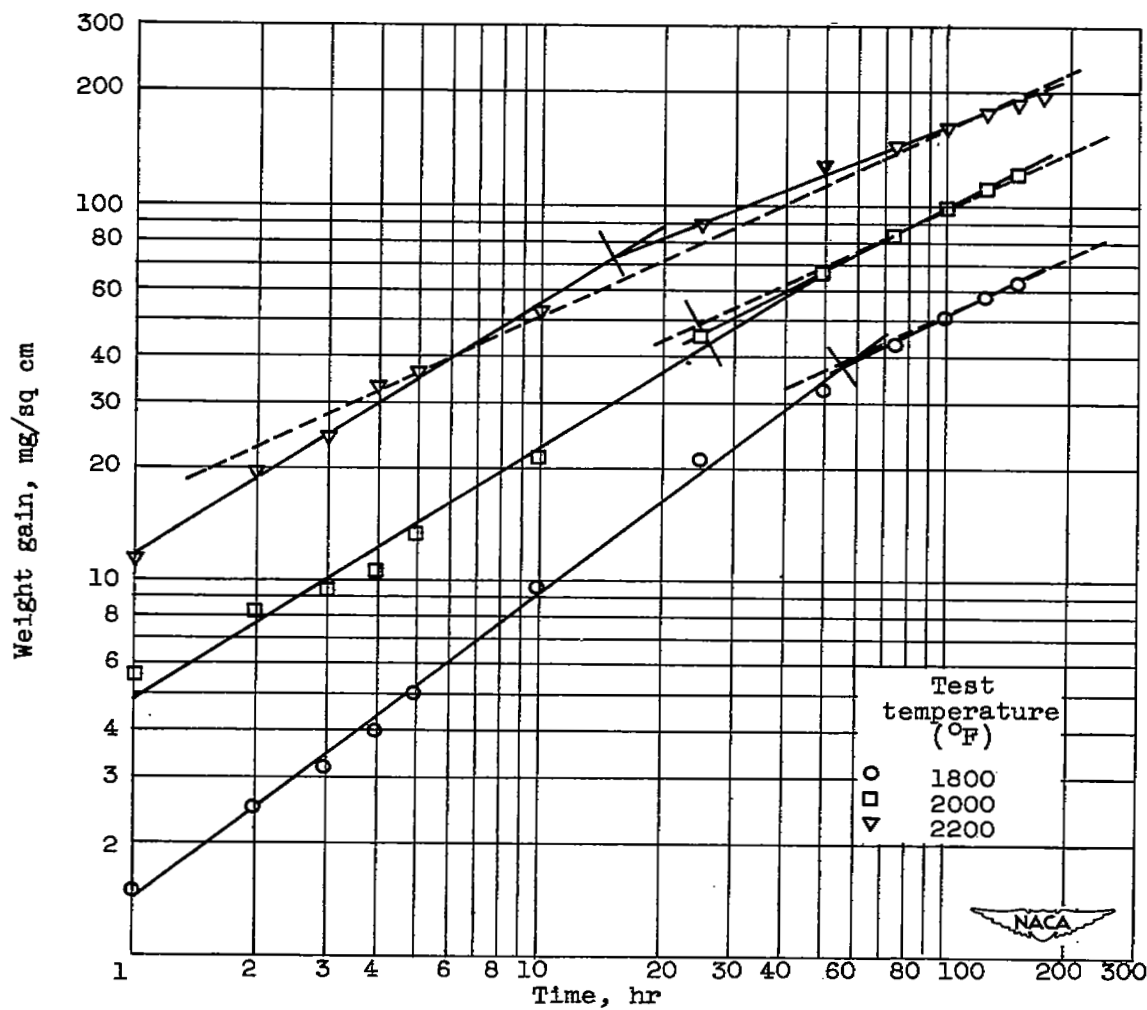


Figure 10. - Oxidation of titanium carbide base ceramals containing 20 weight percent cobalt. (Dashed curves indicate parabolic growth.)

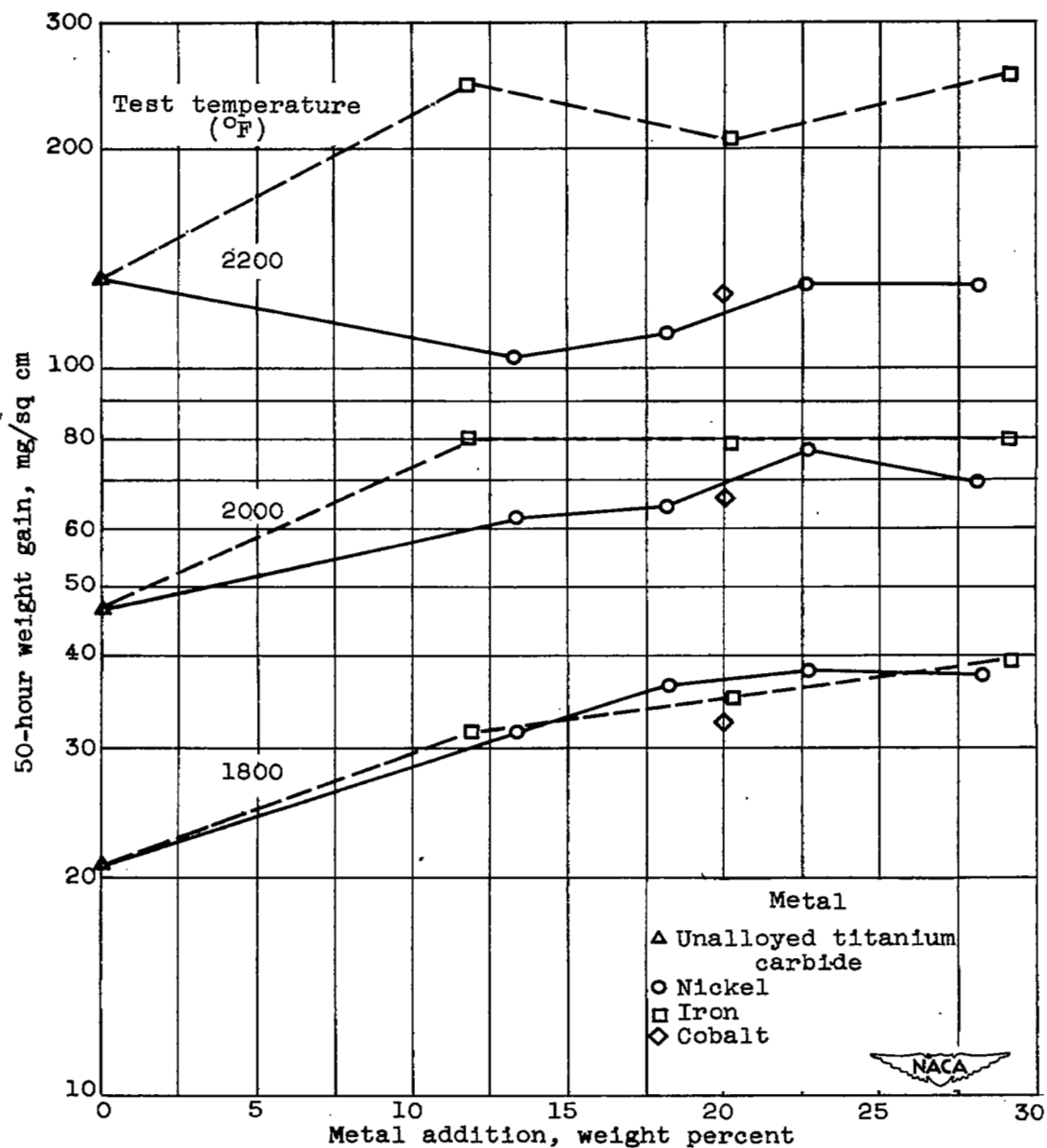


Figure 11. - Effect of metal additions on 50-hour oxidation of titanium carbide base ceramals.

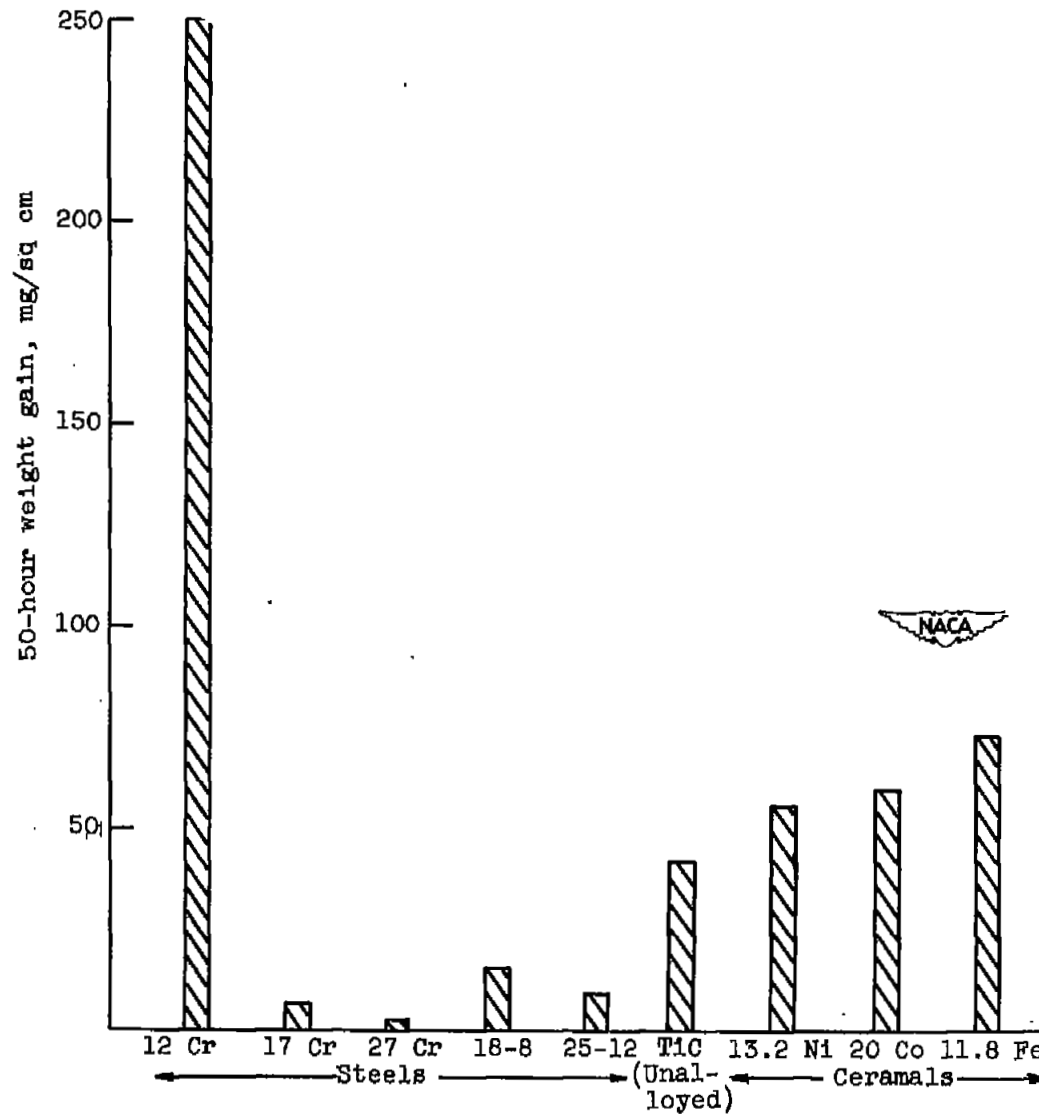


Figure 12. - Comparison of 50-hour oxidation weight gain of titanium carbide and titanium carbide base ceramals with steels at 2000° F.

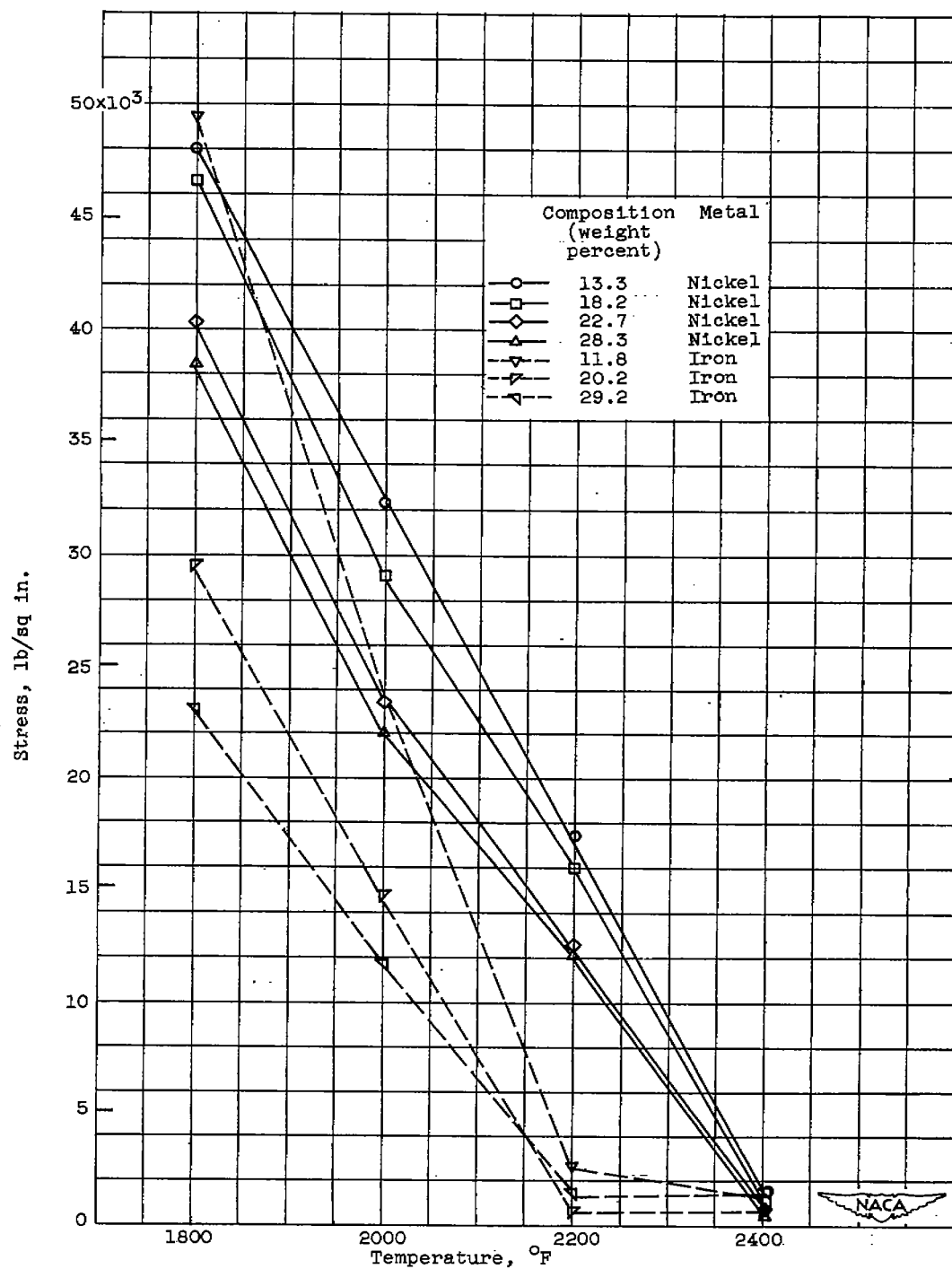
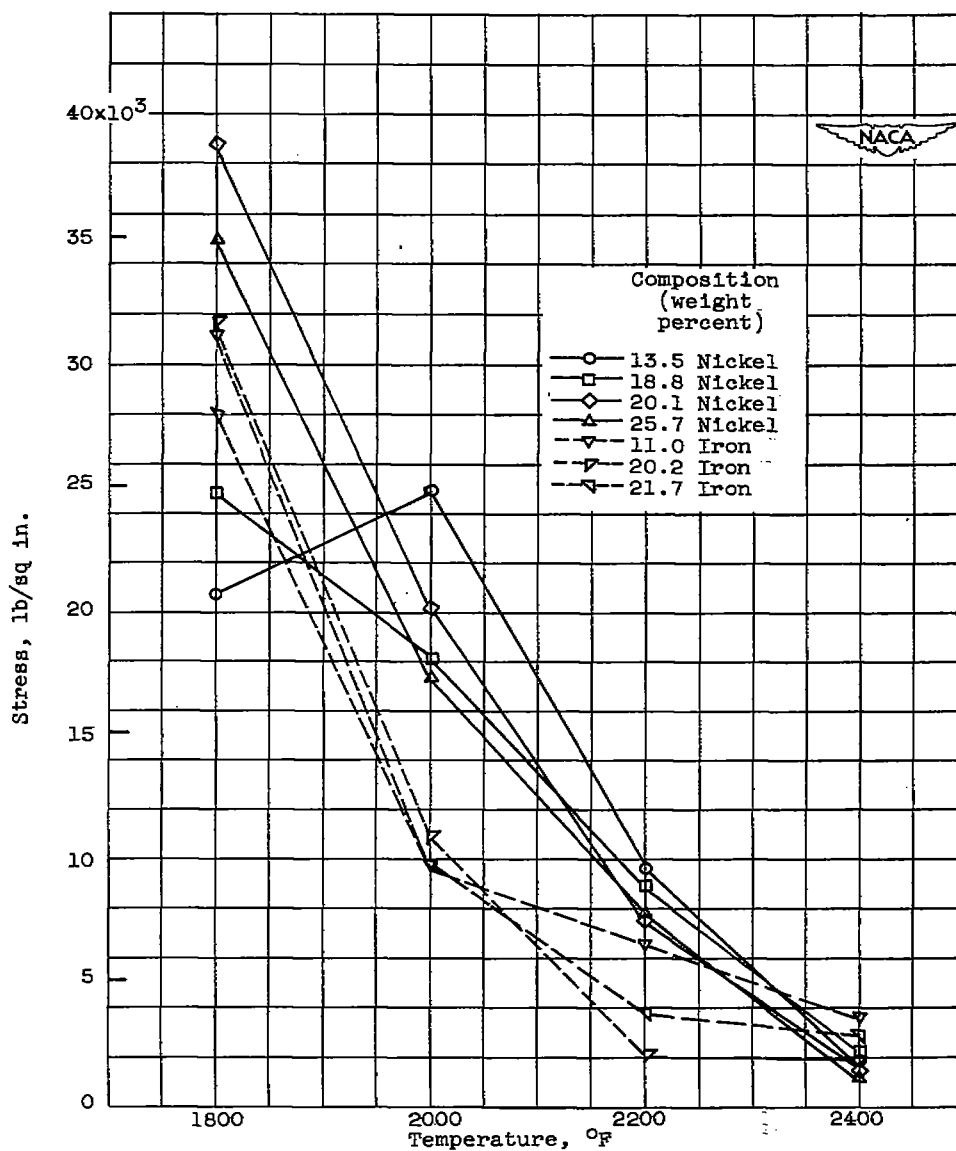


Figure 13. - Effect of temperature upon modulus of rupture of titanium carbide base ceramals.



(b) Hot-press.

Figure 13. - Concluded. Effect of temperature upon modulus of rupture of titanium carbide base ceramals.

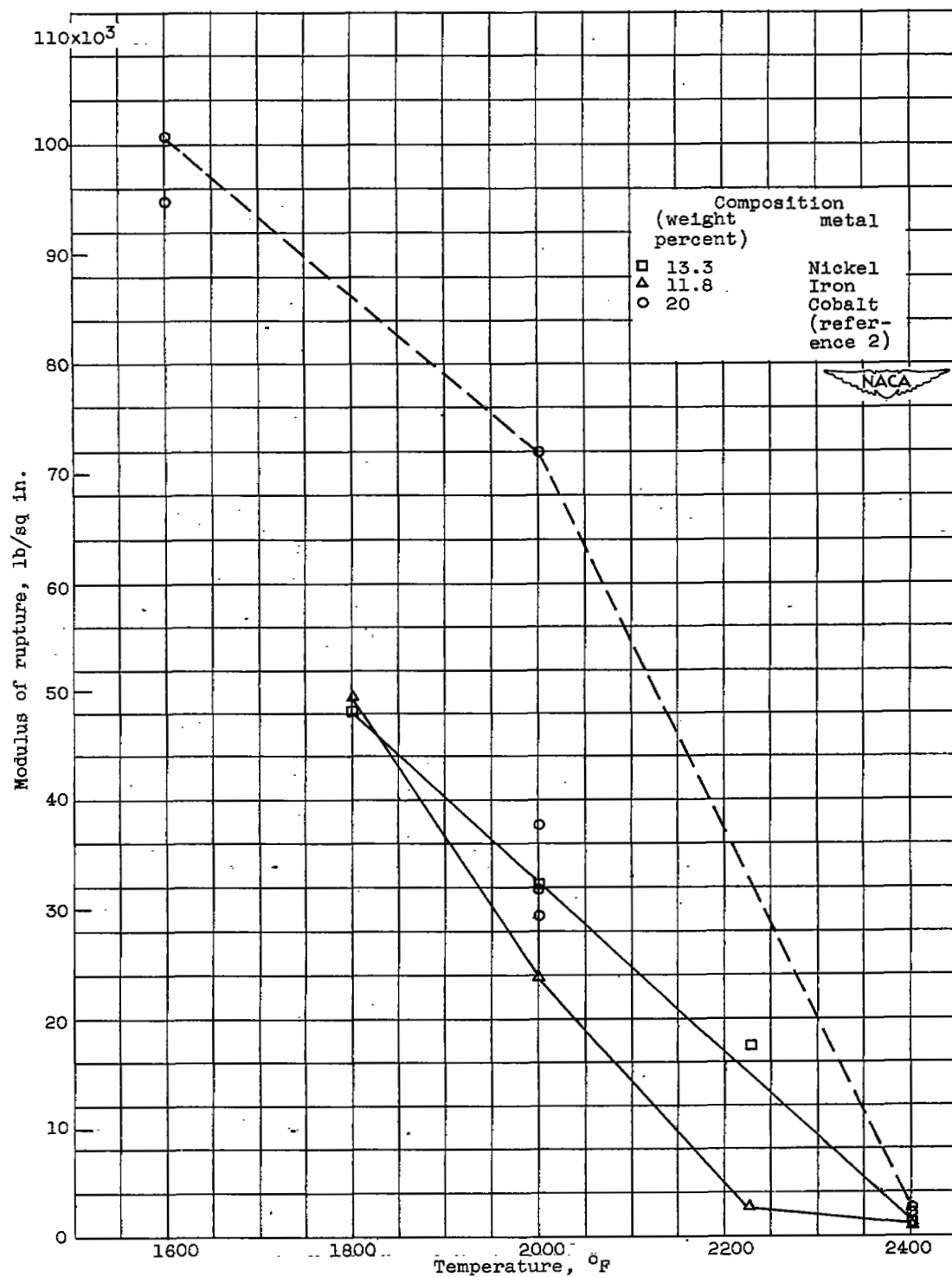


Figure 14. - Comparison of modulus of rupture of titanium carbide base ceramals.

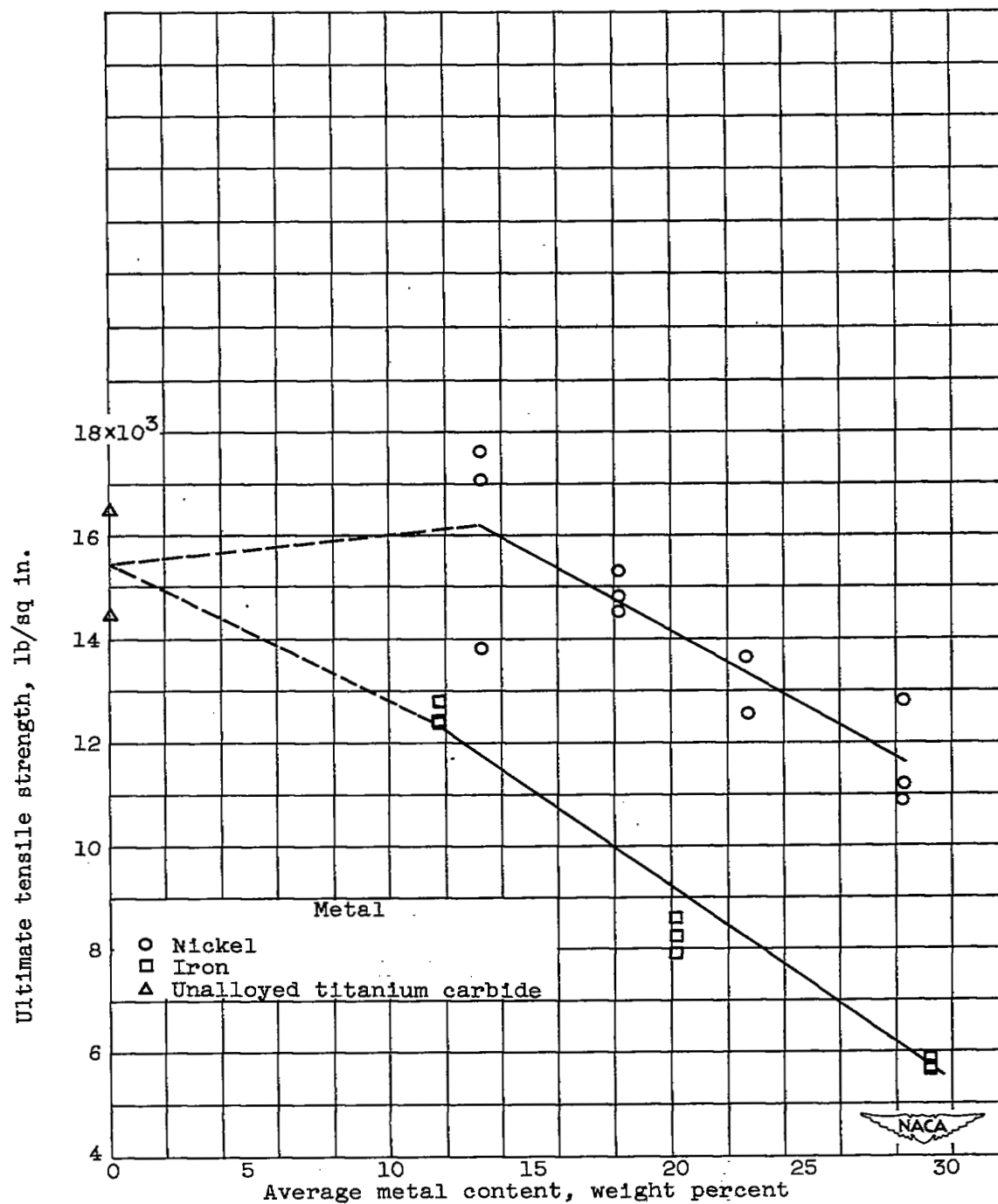
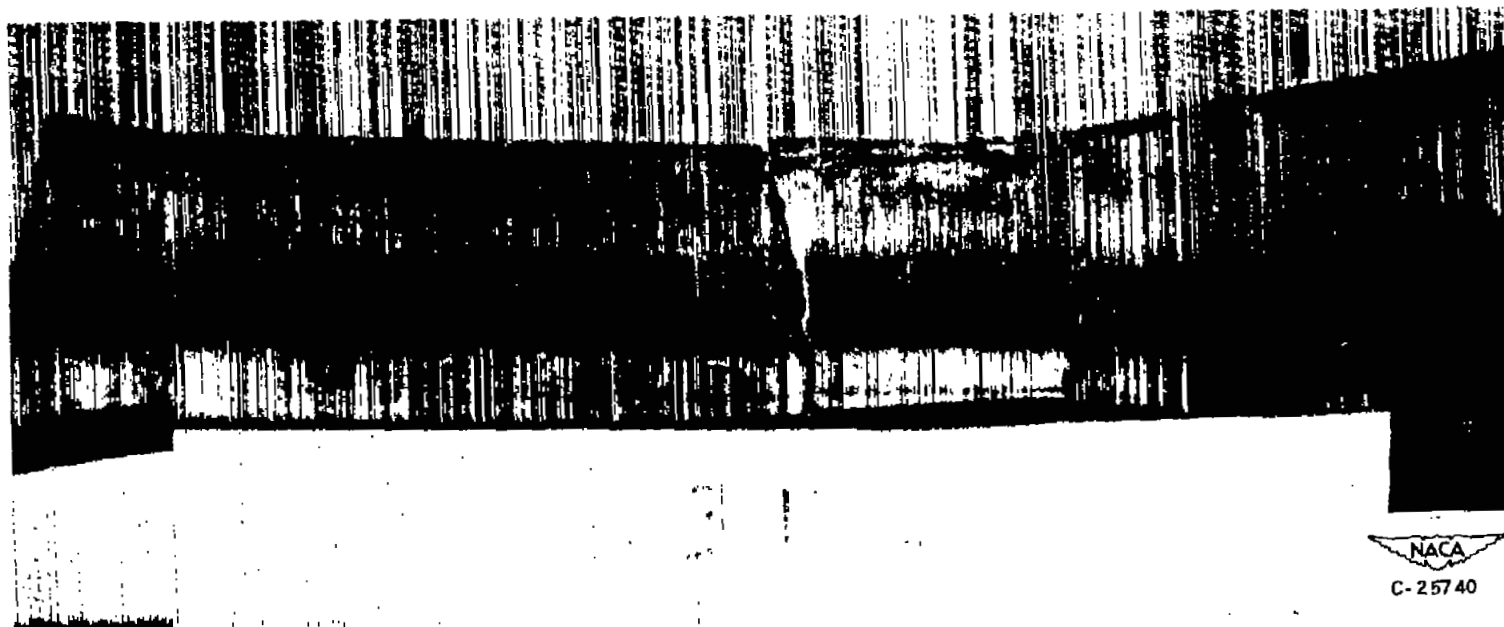


Figure 15. - Tensile strength of titanium carbide base ceramals containing nickel and iron at 2000° F.



NACA
C-25740

Figure 16. - Failure cracks in test section of tensile specimen of titanium carbide base cermet containing 29.2 weight percent (20.5 volume percent) iron. Approximately X4.

NACA RM E51110

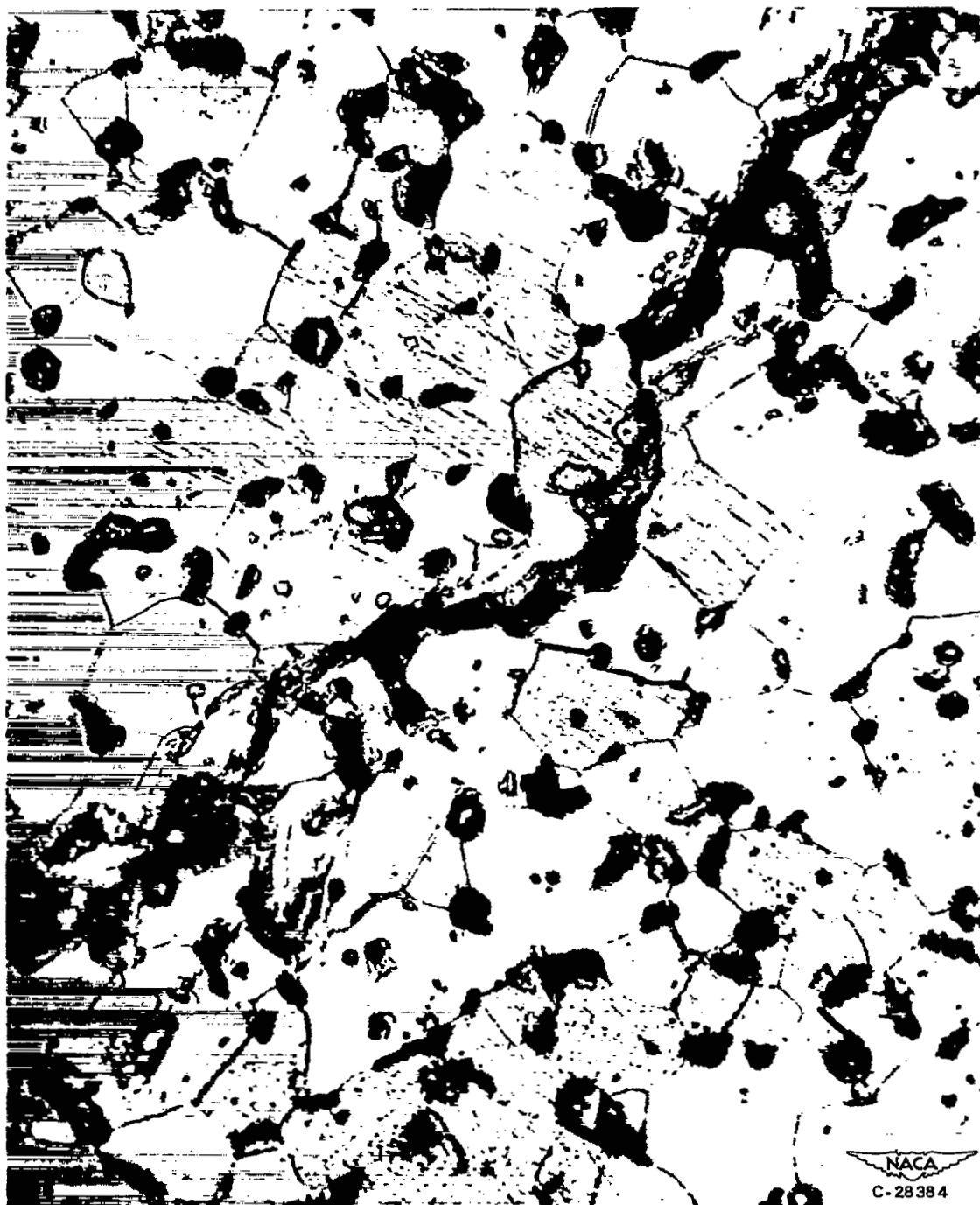
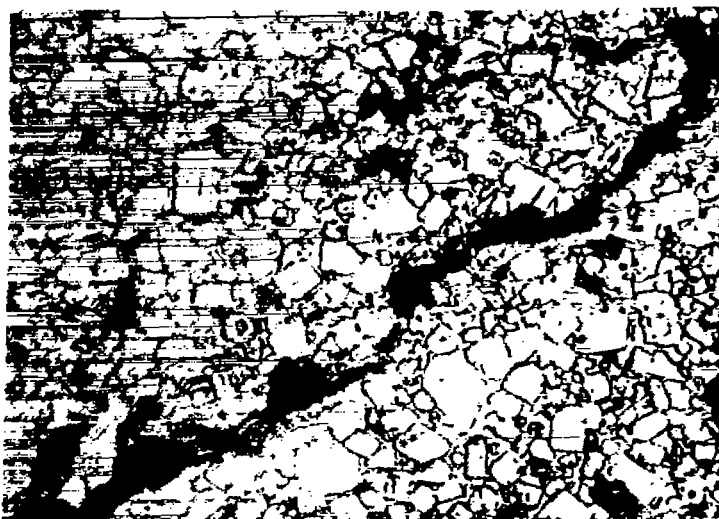


Figure 17. - Fracture path in hot-press 100-percent titanium carbide body tested at 2000° F in tension. Etched with Murakami's reagent. X1500.



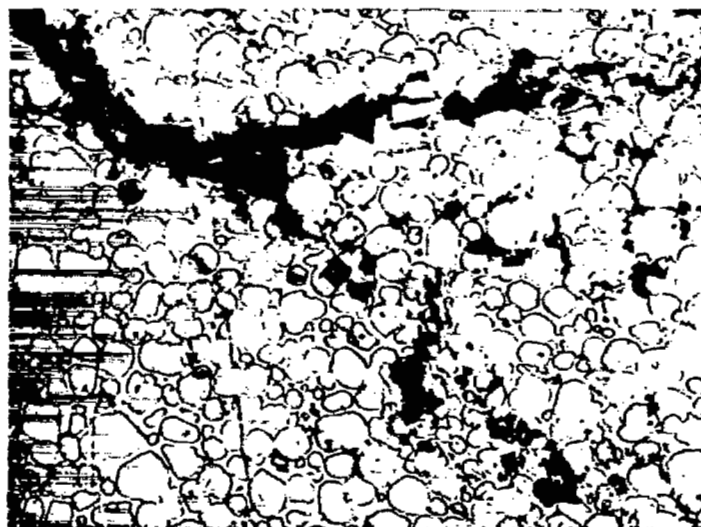
(a) 13.3 weight percent nickel (7.9 volume percent)



(b) 18.2 weight percent nickel (11.1 volume percent)

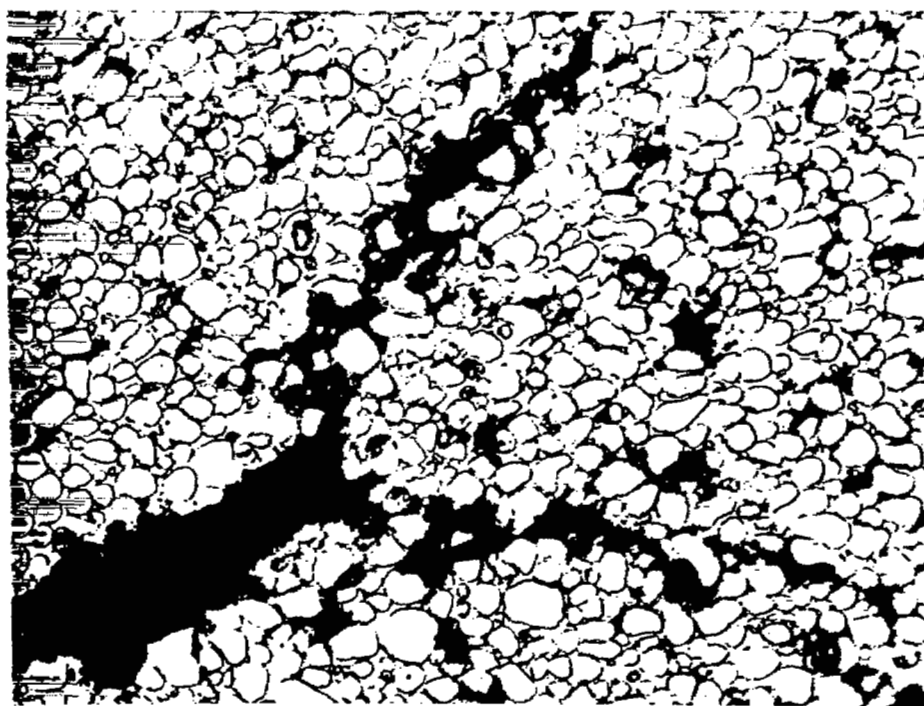
NACA
C-28385

Figure 18. - Internal cracks at tensile fractures in titanium carbide base ceramals containing nickel tested in tension at 2000° F. Etched with Murakami's reagent. X1000.



(a) 20.2 weight percent iron (13.7 volume percent).

NACA
C-28386



(b) 29.2 weight percent iron (20.5 volume percent).

Figure 19.-- Internal cracks at tensile fractures in titanium carbide base ceramals containing iron tested in tension at 2000° F. Etched with Murakami's reagent. X1000.

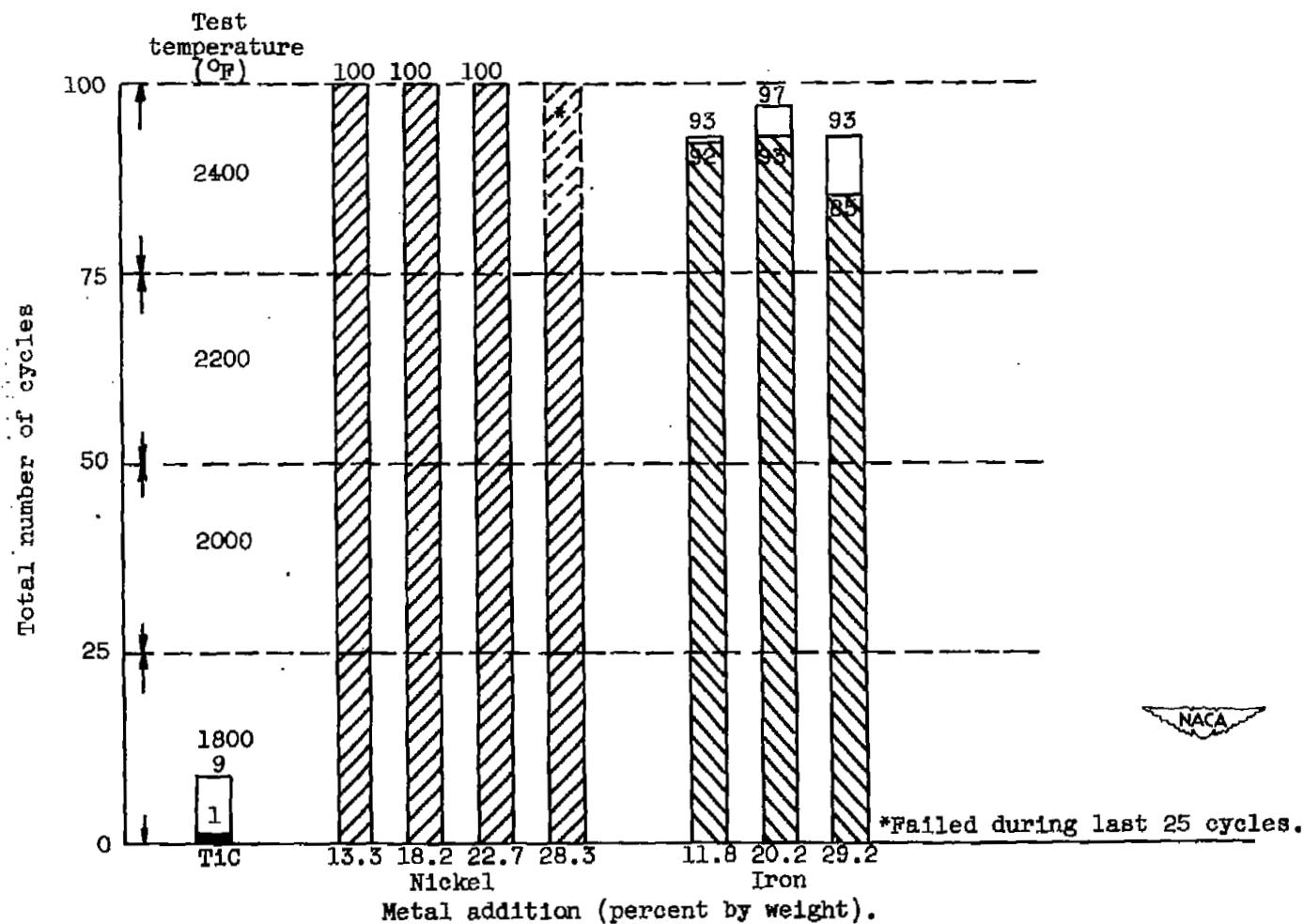
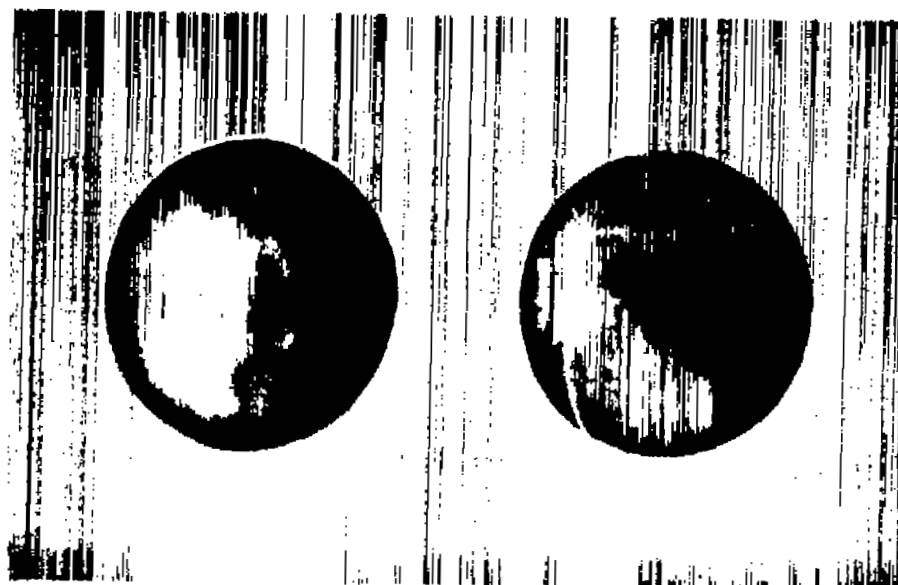


Figure 20. - Thermal-shock resistance of titanium carbide base ceramals air quenched with 50 pounds per minute.



NACA
C-29387

Figure 21. - Internal cracks (network of fine white lines) shown by radiographic inspection of titanium carbide base ceramals containing 28.3 weight percent nickel tested in thermal shock.

3 1773 00019 6159



NASA LEWIS RESEARCH CENTER